FINAL REPORT

PROJECT NO. A-416

AN INVESTIGATION OF TWO-PHASE THERMAL CONDUCTIVITY

by

CLYDE ORR, Jr., and ANDREW McALISTER

CONTRACT NO. DA-01-009-ORD-704

DEPARTMENT OF THE ARMY
U. S. ARMY ORDNANCE DISTRICT
BIRMINGHAM, ALABAMA

DECEMBER 22, 1961

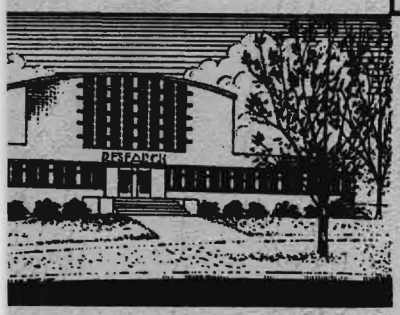

Engineering Experiment Station
Georgia Institute of Technology
Atlanta, Georgia

FINAL REPORT

PROJECT NO. A-416

AN INVESTIGATION OF TWO-PHASE THERMAL CONDUCTIVITY

by

CLYDE ORR, Jr., and ANDREW McALISTER

CONTRACT NO. DA-01-009-ORD-704

DEPARTMENT OF THE ARMY
U. S. ARMY ORDNANCE DISTRICT
BIRMINGHAM, ALABAMA

DECEMBER 22, 1961

TABLE OF CONTENTS

TABLE OF CONTENTS (Continued)

This report contains 111 pages.

LIST OF FIGURES

LIST OF TABLES

LIST OF TABLES (Continued)

LIST OF TABLES (Continued)

I. SUMMARY

This report concerns the thermal conductivity of two-phase systems, one phase dispersed uniformly throughout the other. Three types of dispersions--suspensions (solid particles suspended in a liquid), emulsions (liquid droplets distributed throughout an immiscible liquid), and powder beds (solid particles resting one upon another with a gas filling the interstitial spaces)--were investigated. Previous investigations, equipment information, test procedures, experimental results, and a discussion of results as they relate to theoretical developments and practical uses are included.

A procedure very frequently used in treating theoretically two-phase thermal conductivity is the establishment of a potential field around a single suspended particle and then the superposition of these fields according to some mathematical describable particle layout. The result is generally a series solution of the superimposed potentials. Difficulty with the procedure, however, arises in describing particle shape and orientation in such a way that they can be handled mathematically and yet represent the physical situation. Also, the superposition of the individual potential fields becomes less exact with increasing composition of the suspended phase. Because of these variations it is difficult to determine the reliability of derivations in any specific case. Other analytical schemes are limited in their application because very simplified particle shapes and arrangements have to be assumed for mathematical reasons, and physical systems rarely approach such descriptions. Thus, at best, most derivations are only guides in estimating the thermal conductivity of dispersions. Theoretical developments for powder beds are even more uncertain than

those for suspensions and emulsions.

The portion of this study concerned with suspensions involved an experimental evaluation of the effects of particle properties, such as size, shape, and surface characteristics, as well as the effects of pure phase properties and relative concentrations. Experimental data were collected for glass beads in water (gelled), zinc particles in grease (automobile lubricant), and aluminum in grease suspensions. It was concluded that suspension thermal properties are practically independent of particle size. Likewise, particle surface properties were found to have negligible effects except in cases involving nonwetted surfaces or porous particles. Particle shape, particle concentration, and the separate phase conductivities exert the major influences on suspension thermal conductivities. The empirical equation

$$\frac{k_m}{k_c} = (1 + av_d + bv_d^2) \exp (cv_d),$$

was proposed for predicting suspension thermal conductivities for irregular particles, where k_m and k_c are the thermal conductivities of the mixture and continuous phase, respectively, v_d is the volume fraction of the dispersed phase and a, b, and c are empirical constants. The proposed relationship is adapated to a specific case from generalized graphs that are functions of the pure phase properties and of particle shape. Additional data, however, are needed to test fully this correlation.

Of previously proposed equations, it appears that those immediately following give, in general, the most reliable estimates of particulate suspension thermal conductivities. For a dispersion of spheres, the

equation is

$$\frac{k_m}{k_c} = \left[\frac{2(K_d + 2) + 2(K_d - 1)\, v_d}{2(K_d + 2) - (K_d - 1)\, v_d}\right] \quad \left[\frac{(2 - v_d)(K_d + 2) + 2(K_d - 1)v_d}{(2 - v_d)(K_d + 2) - (K_d - 1)\, v_d}\right] ;$$

for a dispersion of rods oriented in three dimensions, it is

$$\frac{k_m}{k_c} = \left[\frac{(6K_d + 1) + (K_d^2 + 2K_d - 3)v_d}{6(K_d + 1) - 2(K_d - 1)v_d}\right] \quad \left[\frac{6(K_d + 1 - v_d) + (K_d^2 - K_d)v_d}{6(K_d + 1) - (5K_d + 1)v_d}\right] ;$$

and for a dispersion of rods randomly oriented in two dimensions with the long ones perpendicular to the temperature field, the expression is

$$\frac{k_m}{k_c} = \left[\frac{2(K_d + 1) + (K_d + 1)v_d}{2(K_d + 1) - (K_d - 1)v_d}\right] \quad \left[\frac{(2 - v_d)(K_d + 1) + (K_d - 1)v_d}{(2 - v_d)(K_d + 1) - (K_d - 1)v_d}\right] ;$$

where K_d is the ratio of the pure phase thermal conductivities and all the other terms are the same as for the first equation. For suspensions having nearly spherical particles and having pure phase thermal conductivity ratios of over 300, satisfactory results should be obtained from

$$\frac{k_m}{k_c} = 1 - 1.4v_d^{2/3} + 0.4875v_d^{1/3} \left[\frac{\ln(K_d - 1)}{0.25 + (0.403v_d^{-1/3} - 0.5)\ln(K_d - 1)}\right] .$$

In the investigation of emulsions, four systems were studied: carbon tetrachloride-water, hexane-water, diethylbenzene-water, and turpentine-water. Within experimental error, the data showed that emulsion thermal conductivities vary linearly with dispersed phase composition. From this

result and a theoretical investigation of emulsion thermal conductivity, it was concluded that all emulsions behave in this manner except in those extreme cases involving one highly conductive phase. The relationship for predicting emulsion conductivities is

$$\frac{k_m}{k_c} = (1 - v_d) + \frac{k_d}{k_c} v_d$$

The experimental investigation of powder beds employed gas-glass beads as the test systems. A variety of experimental conditions were obtained by varying the size of the glass beads and the type of gas filling the interstices of the bed. The following relationships

$$k_b = \frac{2k_2}{1 - \epsilon^{1/3}} + 4\sigma T^3 e \frac{1}{\epsilon} (1 - \epsilon^{2/3} + \epsilon^{4/3}),$$

$$k_b = \frac{k_g (1 - c)}{(1 - K)\left(\frac{k_g}{k_p}\right) + \frac{1}{\frac{1}{K} + \frac{h_r d}{k_p}}} + c\left(1 + \frac{h_r d}{k_p}\right) k_g,$$

$$\text{and } k_b = \frac{k_g (1 - c)}{(1 - K)\left(\frac{k_g}{k_p}\right) + K} + c\, k_g,$$

based on their generality and the rigorousness of the derivation, are considered, for the present at least, the best available. For them k_b, k_g, and k_p are the thermal conductivities of the bed, gas, and particles, respectively, ϵ is the porosity of the bed; σ is the Stefan-Boltzman constant; e is the

particle emissivity; T is the absolute temperature; d and L are the linear dimensions of the particles, K is an empirical constant, h is the radiation heat transfer coefficient, and c is defined as $1 - \epsilon^{1.3}$. It is not possible to state which of the three immediately preceding equation is the more reliable. From the data generated here the first equation seems far superior. The last equation is merely the preceding equation with radiation made negligible.

II. INTRODUCTION

Problems involving the transfer of heat through dispersed, two-phase systems are frequently encountered in industrial and scientific endeavors. The solution of these problems invariable reduces to a question of the system's thermal conductivity. Since experimental data is very rarely found in handbooks or other information sources, a need exists for appropriate relationships backed by reliable data with which to predict the thermal conductivity of two-phase mixtures.

Reported information at the time this study was initiated provided means for predicting the thermal conductivity of two-phase mixtures only with sufficient accuracy for rather rough calculations. While a number of relationships were proposed in the technical literature both before and during the course of this work, actual data from other sources are still meager. Moreover, nowhere has an attempt been reported to include the effects of degree of dispersion and interfacial phenomena. The objective of this investigation, therefore, was to measure as precisely as possible the thermal conductivity of stable dispersions, being certain that the relative abundance of the various components as well as the physical properties of the dispersed particulates were accurately evaluated. The results were intended to establish which variables were essential in thermal conductivity equations and which were the most reliable relations. New relationships, or modifications of old ones, were to be provided where none was found to be satisfactory. The investigation was to include three types of dispersions: a solid powder in a liquid producing what is called a suspension; liquid droplets in another immiscible liquid, or an emulsion; and a powder bed consisting of a rigid mass of particles with a gas filling the interstices.

III. THEORETICAL BACKGROUND

Thermal conductivity is defined as the constant appearing in the Fourier equation

$$q = k \frac{dt}{dx} \tag{1}$$

where q is the heat flux through an area which is perpendicular to the temperature gradient, dt/dx, and where k is the thermal conductivity. This is the fundamental relationship governing heat transfer by conduction. Application of this basic concept to a general case of heat conduction yields the general heat conduction equation which in Cartesian coordinates is

$$\rho C_p \frac{\partial t}{\partial \tau} = k_x \frac{\partial^2 t}{\partial x^2} + k_y \frac{\partial^2 t}{\partial y^2} + k_z \frac{\partial^2 t}{\partial z^2} + q^1 \tag{2}$$

where ρ, C_p, and k are the density, heat capacity, and thermal conductivity of the conducting medium, respectively, and t the temperature, τ the time, x, y, z the space coordinates, k the thermal conductivity, and q^1 the specific internal heat generation, for instance, the electrical resistance heating. It should be noted that this relationship allows for the dependence of thermal conductivity on direction. Any solution to a heat conduction problem must satisfy this equation. Thus the determination of thermal conductivity must be accomplished by measuring all other terms of this equation or of any integral solution of it. For the case of unidirectional steady state conduction equation 2 simplifies to equation 1.

Due to the extremely complex mechanism of two-phase heat transfer, such analytical expressions as have been developed for expressing thermal conductivity utilize highly idealized models and the results vary with

the degree to which the physical situation is approximated. Most derivations are based on the concept of potential heat flow, which, in itself, is exact and well demonstrated by the complete analogy between electrical conduction and heat conduction. The mathematical procedure is to determine the potential field around a single particulate* and then to superimpose these fields according to some mathematically described arrangement of particulates. The result is generally a series solution of the superimposed potentials. The difficulty with this approach arises in describing the particulate shape and orientation in such a way that the result can be handled mathematically and yet represent the physical situation. Results, however, have been obtained by considering the dispersed phase to be cubes, spheres, flakes, and cylinders in several specifically designated orientations in a continuous medium.

The first investigator to achieve significant results was Maxwell.[1]** He derived an expression for the electrical conductance of a system composed of a single sphere suspended in an infinite medium. Then, by assuming that a suspension of many spheres was still sufficiently dilute to avoid disturbing the field around any one sphere, he developed the result

$$\frac{K_m - 1}{K_m + 2} = v_d \frac{K_d - 1}{K_d + 2} \qquad (3)$$

where K_m is the ratio $(\frac{k_m}{k_c})$ of the mixture thermal conductivity to that of the continuous phase, K_d is the ratio $(\frac{k_d}{k_c})$ of the dispersed phase thermal

*A particulate is either a solid particle or a liquid droplet, and the term is used here to denote either without distinction.

**References are tabulated beginning on page 94.

conductivity to that of the continuous phase, and v_d is the volume fraction of the dispersed phase. In view of the assumptions, the equation is applicable only for small values of v_d, and is exact only for $v_d = 0$. Even though the final result itself is limited, the concepts used in its derivation provided the ground work for other investigators.

Lord Rayleigh[2] studied the limiting assumptions involved in Maxwell's derivation and proposed an arrangement to remove the condition that the distance between the particulates be large. He developed two series expansions with interdependent coefficients which described the overall potential field in terms of the superimposed fields when the spheres were arranged in a cubic lattice. For the case of spheres this led to

$$K_m = 1 - \frac{3v_d}{\frac{2 + K_d}{1 - K_d} + v_d + 1.65 \frac{K_d - 1}{K_d + 4/3} v_d^{10/3}} \qquad (4)$$

where the symbols are as previously defined for equation 3. The above expression has the added advantage that it is theoretically valid for all values of v_d. Thus it has more utility than the Maxwell equation. It has the disadvantage that it is restricted to a cubical lattice arrangement of spheres. In reality, this is not the exact physical condition in a dispersion but this condition is approached. As was done for a dispersion of spheres, Lord Rayleigh also developed an expression for cylinders arranged in a cubical lattice with the potential field perpendicular to the longitudinal axes. This resulted in

$$K_m = 1 - \frac{2v_d}{\frac{1 + K_d}{1 - K_d} + v_d - 0.3058 \frac{1 - K_d}{1 + K_d} v_d^4} \qquad (5)$$

where the equation has the same limitations as the one for a dispersion of spheres.

In a later study, Runge[3] found the Lord Rayleigh equation for spheres to contain an error. The corrected expression is

$$K_m = 1 - \frac{3v_d}{\frac{2 + K_d}{1 - K_d} + v_d + 0.525 \frac{K_d - 1}{K_d + 4/3} v_d^{10/3}} \tag{6}$$

The results of Maxwell and Lord Rayleigh are restricted to uniform size particulates, which, of course, is almost never the case actually. Bruggerman[4] modified the Maxwell equation by expanding it in a Taylor's series and treating the first two terms with an integral technique. The result was

$$1 - v_d = \frac{K_m - K_d}{K_m^{1/3} (1 - K_d)} \tag{7}$$

The model imposed by these mathematical operations was that each spherical particulate be a different size from its nearest neighbor particle, the difference being such that the distortion of the potential field due to the smaller particulates was negligible. A descriptive quantity for the size distribution does not appear in the equation, since this was predetermined by the mathematics and cannot be varied. This expression has the advantage that it does take account of, to some extent at least, the effect of particulate size distribution, but it is still limited to small values of v_d.

While the Bruggerman equation is valid only for spheres, Meredith[5]

obtained a similar result which may be adapted to a variety of particle shapes. This development was based on the Burgers[6] equation, which in ellipsoidal coordinates is

$$K_m = 1 - \frac{v_d(1 - K_d)}{3} \sum_i \frac{1}{1 - (1 - K_d) L_i} \tag{8}$$

where $L_i = \frac{abc}{2} \int_0^\infty \frac{d_\eta}{(\eta + a^2)R_\eta}$

and $R_\eta = [(\eta + a^2)(\eta + b^2)(\eta + c^2)]^{1/2}$

in which the terms a, b, c designate the length of the semiprincipal axes of the ellipsoid, and the parameter η gives a family of ellipsoids all confocal with the body where $\eta = 0$. The subscript i refers to the component of the potential field in the i direction. Like Maxwell's approach, this development was derived by solving the potential field about a given particulate. In this case, confocal ellipsoidal coordinates were used so that particle shapes other than spheres could be considered. By expanding this result into a Taylor's series, Meredith obtained

$$(1 - v_d) = \left(\frac{K_m - K_d}{1 - K_d}\right) \left(\frac{K_m + \alpha K_d}{1 + \alpha K_d}\right)^\gamma (K_m)^\beta \tag{9}$$

which is valid for various particle shapes depending on the value of the constants α, β, and γ. For spheres α, β, and γ are 0.500, -0.333, and 0.000, respectively; likewise for rods 0.200, 0.000, and -0.400; and for disks 2.000, 0.000, and 1.000. Although the equation takes into account particle shape, it is still theoretically limited to small values of v_d.

Meredith made several other contributions to the theoretical development of two-phase conduction. One was the determination of one additional term of the series in the Lord Rayleigh equation. The result was

$$K_m = \frac{\frac{2 + K_d}{1 - K_d} - 2v_d + 0.409 \frac{6 + 3K_d}{4 + 3K_d} v_d^{7/3} - 2.133 \frac{3 - 3K_d}{4 + 3K_d} v_d^{10/3}}{\frac{2 + K_d}{1 - K_d} + v_d + 0.409 \frac{6 + 3K_d}{4 + 3K_d} v_d^{7/3} - 0.906 \frac{3 - 3K_d}{4 + 3K_d} v_d^{10/3}} \quad (10)$$

Another development by Meredith is based on the fact that the thermal conductivity of the continuous phase in the region of a particulate is better represented by the conductivity of the mixture as a whole than by the thermal conductivity of the continuous phase alone. With this in mind, Meredith envisioned as a model a dispersion of equally sized particulates in high concentration with respect to the dispersed phase. Under these conditions the temperature field around any one particulate is influenced by all others in the suspension. This situation was approximated by the assumption that the properties of the continuous phase surrounding a particulate were primarily a function of the neighboring particulates; other particulates were considered to have a negligible effect. The neighboring particulates, on a statistical basis, were conceived to be in a spherical array at a given radius from the particulates being considered. The radius was determined by the suspension or emulsion concentration. These assumptions defined a region of space in a given suspension which can be described mathematically. A continuation of this development from a statistical point of view resulted in the following expression for spheres

$$K_m = \left[\frac{2(K_d + 2) + 2(K_d - 1)\, v_d}{2(K_d + 2) - (K_d - 1)\, v_d}\right] \left[\frac{(2 - v_d)(K_d + 2) + 2(K_d - 1)\, v_d}{(2 - v_d)(K_d + 2) - (K_d - 1)\, v_d}\right] \quad (11)$$

For a dispersion of rods randomly oriented in three dimension, it gave

$$K_m = \left[\frac{6(K_d + 1) + (K_d^2 + 2K_d - 3)\, v_d}{6(K_d + 1) - 2(K_d - 1)\, v_d}\right] \left[\frac{6(K_d + 1 - v_d) + (K_d^2 - K_d)\, v_d}{6(K_d + 1) - (5K_d + 1)\, v_d}\right] \quad (12)$$

and for a dispersion of rods randomly oriented in two dimensions with the long axes perpendicular to the temperature field, there resulted

$$K_m = \left[\frac{2(K_d + 1) + (K_d - 1)\, v_d}{2(K_d + 1) - (K_d - 1)\, v_d}\right] \left[\frac{(2 - v)(K_d + 1) + (K_d - 1)\, v_d}{(2 - v)(K_d + 1) - (K_d - 1)\, v_d}\right] \quad (13)$$

Meredith also investigated the effect of solid particle agglomeration. Mathematically, the mechanics of agglomeration are extremely complicated; however, it was possible to describe the combination of spherical particles to form a doublet. Again, a statistical approach was used, the basis for this derivation being the fact that the time average volume concentration of two unit inelastic collisions (doublets) in a suspension of spherical particles is four times the square of the single particle concentration. With this information and the fact that a doublet of spheres has roughly the character of a probate spheroid with a 2:1 axial ratio, the following expression was derived for the conductivity of such a mixture

$$K_m = \frac{6(3 + K_d) - 2(1 - K_d)\left[(1 + 16v_d)^{1/2}\ (1 - N) + (1 + 8v_d)\, N\right]}{3(5 + 3K_d) + (1 - K_d)\left[(1 + 16v_d)^{1/2}\ (1 - N) + (1 + 8v_d)\, N\right]} \quad (14)$$

where $N = 1.18 \dfrac{(K_d + 2.00)(K_d + 2.96)}{(K_d + 4.81)(K_d + 1.41)}$

The developments previously discussed dealt principally with the mathematical analysis of conduction. A different approach was proposed by Weiner.[7] He showed that

$$K_m = v_d K_d + (1 - v_d) \tag{15a}$$

and

$$\frac{1}{K_m} = \frac{v_d}{K_d} + (1 - v_d) \tag{15b}$$

define the limits between which suspension or emulsion conductivity can vary. These equations represent the equivalent thermal conductivity of a laminated configuration with the heat flow, respectively, parallel and perpendicular to the laminations. The equivalent conductivity of any suspension or emulsion could be expressed by combining these two extremes. Wiener proposed a linear combination of these equations for representing this intermediate value. Thus

$$\frac{k_m}{k_m + u} = \frac{v_d k_d}{k_d + u} + \frac{1 - v_d}{k_c + u} \tag{16}$$

where u is a constant to be determined experimentally. This number should be characterized by particulate shape, particulate size, and the relative properties of the two phases forming the mixture.

Lichtenecker[8] proposed a similar approach except the logarithmic equation for conduction was chosen

$$\ln(k_m) = v_d[1 + 6(1 - v_d)] \ln k_d + (1 - v_d)(1 - u\, v_d) \ln k_c \qquad (17)$$

This equation was found to describe most of the data available at that time. Again u was a characteristic constant determined by experiment.

Jefferson, et al.,[9] derived an expression for calculating equivalent two-phase thermal conductivities by applying the elementary concepts of thermal conduction to a model composed of a suspension subdivided into smaller cubes, each containing a solid particle. The solid particles were assumed to be spherical and uniform in size. It was further assumed that the conductivities and densities of both solids and fluid were constant and that the ratio of k_d/k_c was very large. With these assumptions, the suspension thermal conductivity was found to be

$$K_m = 1 - 1.21\, v_d^{2/3} + 0.4875\, v_d^{1/3} \left[\frac{(\ln k_d - 1)}{0.25 + (0.403\, v_d^{1/3} - 0.5)(\ln k_d - 1)}\right] \qquad (18)$$

Equations 1 through 18 are applicable only to cases where the dispersed particulates are not in contract with each other; they must be completely surrounded by the continuous medium. Therefore, to describe the thermal conductivity of a bed of powder, which is a two-phase system in which particles do contact one another, a different type of equation allowing for particle contact must be used. Furthermore, gases behave much differently from liquids with respect to pressure. This behavior is due to the change of mean free path of gas molecules with pressure.

The difficulty in calculating the thermal conductivity of a system composed of particles interspersed with a continuous gas phase lies both

in formulating a model that represents the system and in expressing mathematically effective conductivity on the basis of the system. The model must inevitably be complicated, particularly if irregular particles of varying sizes are considered, but the effective conductivity is even more complicated unless simple geometries or analyses based on highly unreasonable assumptions are employed.

Early attempts at establishing particle bed conductivities made use direcly of Maxwell's and Lord Rayleigh's equations. As will be recalled, these expressions assume particles located at the center of unit cubical spaces. Since this does not even correspond approximately to the actual situation, it is not surprising that poor agreement was attained. By assuming cubes in a cubical array and adding the limitation that heat must flow in such a manner that points of equal temperature--isotherms--are located in planes perpendicular to the direction of heat flow, Russell[10] obtained

$$k_b = k_g \left[\frac{(k_p/k_g)\, v_d^{2/3} + (1 - v_d^{2/3})}{(k_p/k_g)\,(v_d^{2/3} - v_d) + (1 - v_d^{2/3} + v_d)} \right] \qquad (19)$$

where k_b denotes the bed's effective conductivity, k_g the gases' conductivity, and k_p and v_d the particles' conductivity and volume fraction, respectively, as before. As written, the expression is not to be recommended; with modifications to include radiation and gas pressure effects, as described subsequently, it is somewhat more useful. Other relationships of both lesser and greater complexity but still involving only the two component conductivities and their proportion have been devised by Deissler

and Eian,[11] Strickler,[12,13] and Woodside.[14]

A semiempirical graphical correlation of Deissler and Eian and by Deissler and Boegli[15] is one of the most readily useful for powder bed conductivity. It is reproduced in Figure 1. For gases at normal pressures and moderate temperatures the correlation appears to be one of the best.

Any correlation to apply adequately over a range of conditions must account for variations in gas temperature, gas pressure, and particle size. With ordinary temperatures, atmospheric pressure, and particle sizes between -28 and +325 mesh, thermal conductivities were found by Marathe and Tendolkar[16] to be independent of the actual value of the size as long as the masses' porosity was held constant. On the other hand, thermal conductivities were found to vary linearly with porosity, increasing as the apparent density rose. At high temperature, radiation effects become very important, particularly if the particles are relatively large. For 1 mm particles this temperature is reached at about 400°C, while for 0.1 mm particles it may be as high as 1500°C. When the dimensions of the gas spaces become of the same order as the mean free path of the gas molecules, thermal conductivity is further changed. Since much of the conduction through powders occurs across points of contact between particles and those portions of particles nearest contact, this shift may even become significant when the particle diameter is about 1000 times the mean path length. It registers as a decrease in conductivity and occurs because gas molecules can cross from one surface to another under this condition before reaching thermal equilibrium. There is thus an abrupt change of temperature from the surface to the gas instead of the gradual transition that exists at higher pressures. The pressure at which it becomes necessary

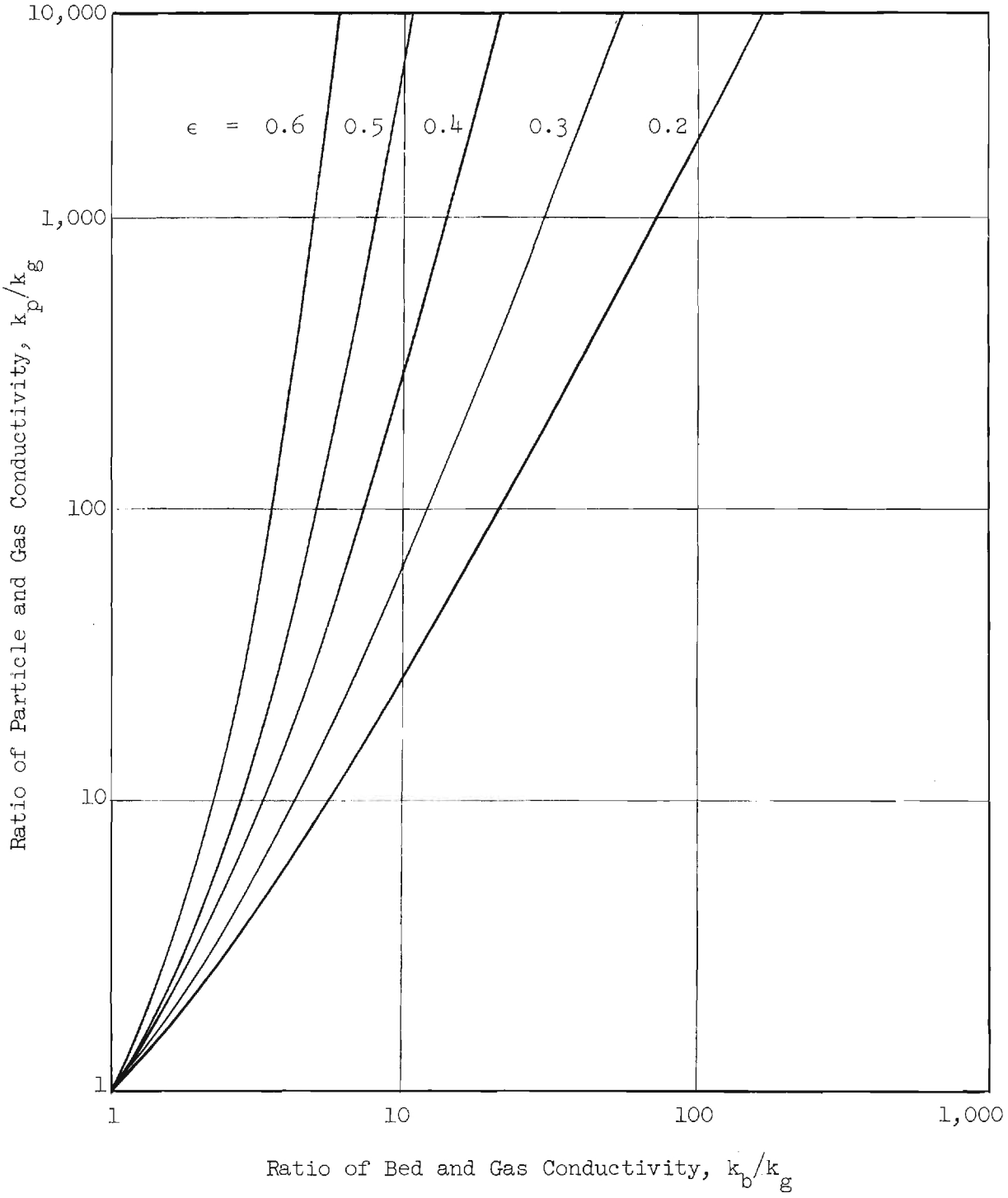

Figure 1. Deissler and Eian[11] Correlation for the Thermal Conductivity of a Packed Bed with Gas Filling the Interstices.

to correct for the change in gas conductivity is called the break-away pressure, designated P_{b-a}. An equation relating break-away pressure, temperature, and particle size is given by Deissler and Eian as

$$P_{b-a} = 1.77 \times 10^{-21} \left(\frac{T}{dm^2} \right) \tag{20}$$

where P_{b-a} is measured in lb/ft^2, the absolute temperature T in ^{o}R, d the particle diameter in ft, and m the mean diameter of the gas molecule in ft. When the gas pressure within a powder mass is less than that calculated from equation 20, the apparent gas conductivity should be calculated, according to Schotte,[17] by the equation

$$k_{ag} = \frac{k_g}{1 + 2.03 \times 10^{-22} \left(\frac{C_p/C_v}{1 + C_p/C_v} \right) \left(\frac{1 - \epsilon}{\epsilon} \right) \left(\frac{T\, k_g}{Pdm^2\, C_p\, \mu} \right)} \tag{21}$$

where k_{ag} is the apparent gas conductivity in BTU/hr ft ^{o}F, k_g the normal gas conductivity, also in BTU/hr ft ^{o}F, C_p the gas heat capacity at constant pressure in BTU/lb ^{o}F, C_p/C_v the ratio of gas heat capacity at constant pressure to the heat capacity at constant volume, ϵ the powder's porosity, P the gas pressure in lb/ft, d the particle diameter in ft, μ the gas viscosity in lb/hr ft, and T and m as given above. Allowance for the contribution of radiation within a powder is made, according to Schotte, by estimating the bed's conductivity by the graphical correlation of Deissler and Eian, using, if necessary, the above equation for apparent gas conductivity and then adding the conductivity attributable to radiation k_r given by

$$k_r = 0.692\ ed\ (T^3/10^8) \tag{22}$$

where k_r is in BTU/hr ft $^{\circ}$F, e the particle emissivity, and other terms as previously used. This correlation is supported by the data of Yagi and Kunii[18] which relates to iron spheres, porcelain cylinder and granules, cement clinker, and fire-brick particles in the 800°C range. The correlation should not be applied outside the limits over which it has been tested. Presently this is for porosities between 0.2 and 0.6, and values of the ratio k_p/k_g of less than 6000.

Other correlations attempting to account for radiation effects have been presented by Laubitz.[19] Using the basic model described by Russell but assuming uniform cubes scattered randomly in cubical volumes, except that corresponding faces of the cubes remain parallel, the relationship for k_r is found

$$k_r = 4\sigma\ T^3 e\ \frac{L}{\epsilon}\ (1 - \epsilon^{2/3} + \epsilon^{4/3}) \tag{23}$$

where k_r is the conductivity component due to radiation, σ the Stefan-Boltzmann constant, T the absolute temperature, e the particle emmissivity, L the linear dimension of the particles (assumed to be cubes), and ϵ the porosity. Equation 23 added to twice the conductivity calculated from equation 19 gives the effective conductivity of the powder-gas mass if the particles are essentially of one size, according to the findings of Laubitz's investigation. Twice the conductivity of equation 19 is specified because with this factor good agreement was obtained when the correlation was checked against experimental data for alumina and zirconia beds between 100° and 1000° C. Powders with a considerable spread of particles

were not well correlated by the relationship and it should be applied with caution to materials other than those mentioned. When the particle conductivity is large in comparison to the gas conductivity, the equation above combined with equation 19 can be simplified to

$$k_b = \frac{2k_g}{1 - \epsilon^{1/3}} + 4\sigma T^3 e \frac{L}{\epsilon} (1 - \epsilon^{2/3} + \epsilon^{4/3}) \qquad (24)$$

Considering a powder mass to be three components of different conductivity--the powder and interstitial gas, the contacting path through the powder, and the interstitial fluid--arranged in parallel, Kimura[20] proposed the relationship

$$k_b = \frac{k_g (1 - c)}{[(1 - K)(k_g/k_p) + 1/(1/K + h_r\, d/k_p)]} + c (1 + h_r\, d/k_p)\, k_g \qquad (25)$$

with k_b, k_g, k_p, and d as used previously with conductivities measured in kcal/m hr $^{\circ}$C and particle diameter in meters; c defined as $1 - \epsilon^{1.3}$, where ϵ is the bed porosity; h_r a radiation heat transfer coefficient defined as equal to $0.195\ (T/100)^3$ in units of kcal/m^2 hr $^{\circ}$C when T is $^{\circ}$K; and K a constant as determined by Table 1. This correlation was established using the investigator's own experimental data and data from numerous other sources. It included lead and steel spheres in air, methane, propane, carbon dioxide, and hydrogen; silicon carbide particles in air, carbon dioxide, hydrogen, and helium; calcite particles in air; and quartz powder in air. Comparison of values with experimental data from still other sources for glass spheres, celite cylinders, coal particles, sand, alumina

TABLE I

DIMENSIONLESS CORRELATION FOR CONSTANT K APPEARING IN EQUATIONS 25 AND 26 IN TERMS OF THE RATIO OF GAS CONDUCTIVITY TO PARTICLE CONDUCTIVITY AND POROSITY*

Conductivity Ratio (k_g/k_p)	$K\epsilon^{1.5}$
5×10^{-4}	0.13
1×10^{-3}	0.19
5×10^{-3}	0.33
1×10^{-2}	0.38
5×10^{-2}	0.48
1×10^{-1}	0.50
5×10^{-1}	0.53
1	0.51

*For source see reference 21.

powder, and marble granules all in air, the particles ranging from 22μ to 16.5 mm in diameter and temperatures up to 300°C, gave agreement within 10 per cent in the majority of cases but several values differed by 50 per cent and a few more than 100 per cent. Near room temperature the previous equation reduces simply to

$$k_b = \frac{k_g (1 - c)}{(1 - K)(k_g/k_p) + K} + ck_g \qquad (26)$$

since radiation effects are negligible under these circumstances. Neither of the two previous equations should be used outside the range of conditions indicated.

Other Japanese investigators, notably Sugiyama and Fujitsu,[21] used an electric analog method to arrive at an extremely complicated relationship. Even though it may readily be solved with the aid of graphs provided by the investigators, it does not appear to be as acceptable as an earlier result of Yagi and Kunii. This earlier study is particularly significant because of the analytical way in which the problem was approached. The basic model was suggested by Ranz.[22] Here heat is considered as passing through a powder bed by paths each composed of one or more discrete steps involving (1) the solid, (2) the contact surface of the solid, (3) radiation between solid surfaces, (4) radiation between adjacent voids, and (5) the gas film near points of contact between the solids. A summation of heat flow along each path is found to result in a general equation which can be simplified for special cases and adapted to particles that are spheres, cylinders, or approximations of such

shapes. The equation becomes, in the case of particles with gas-filled interstices,

$$k_b = \frac{k_g (1 - \epsilon)}{(k_g/k_p) + 1/[(1/\phi) + (d\, h_{rp}/k_g)]} + \epsilon dh_{rv} \qquad (27a)$$

particles in a vacuum

$$k_b = k_p \delta + \frac{k_p (1 - \epsilon)}{1 + k_p/(dh_{rs})} + \epsilon\, dh_{rv} \qquad (27b)$$

and very fine particles and gas filled spaces

$$k_b = \frac{k_g (1 - \epsilon)}{k_g/k_p + \phi} \qquad (27c)$$

In these equations, k_b, k_g, and k_p are as defined previously and measured in kcal/m hr ^{o}C, d the average particle diameter in meters, ϵ the bed porosity, δ the fractional area in perfect particle contact, ϕ the effective thickness of the fluid near points of contact between particles divided by the particle diameter, and h_{rs} and h_{rv} radiation coefficients for transfer between solids and between gas spaces, respectively, expressed in units of kcal/hr m^2 ^{o}C by

$$h_{rs} = 0.1952 \left(\frac{e}{2 - e}\right) \left(\frac{T}{100}\right)^3 \qquad (28a)$$

and

$$h_{rv} = \frac{0.1952}{1 + \left[\frac{\epsilon}{2(1 - \epsilon)}\right] \left(\frac{1 - e}{e}\right)} \left(\frac{T}{100}\right)^3 \qquad (28b)$$

where e is the solid emissivity and T the temperature in ^{o}K. The term δ is presently unpredictable; it must be determined experimentally for each system under at least one set of conditions and then applied with other conditions. Essentially the same data were used in establishing this correlation as in those previously presented, with the exception of high temperature data taken by Sugiyama and Fujitsu.

When the particle bed consists of very small and loosely packed particles, more heat may be conducted across it by the gas than by the particles. The effect of reducing the gas pressure is then quite noticeable. In fact, the particles under this low pressure condition actually reduce heat transfer by preventing direct radiation across what otherwise would be a void space. Powder-filled, but evacuated, spaces are of considerable current interest for insulating liquefied gas containers and other low-temperature devices.

According to Weininger and Schneider,[23] if the gas pressure in a bed of powder is increased rather than reduced, conductivities rise slightly more than would be predicted on the basis of the pressure coefficient of thermal conductivity for the gas alone. In some cases, the difference can be quite considerable. This behavior probably is attributable to an increased adsorption of the gas on the solid material as pressure rises.

IV. EXPERIMENTAL WORK

A. Apparatus

1. Means for Determining Thermal Conductivities

There are two basic approaches for making thermal conductivity determinations. One utilizes unsteady state conduction and the other employs the steady state. The unsteady state approach involves a situation in which the heat flux varies with time, the variation being completely arbitrary. For simplicity, however, the time dependence of this heat flux is generally predetermined to aid in the interpretation of the experimental data. The procedure is to make temperature measurements for a given region within the conducting medium in order to establish temperature as a function of both time and position for a given time interval. This is accomplished by measuring temperatures at a sufficient number of times and positions to construct smooth curves of these relationships. From these curves the necessary derivatives for equation 2 are determined with either graphical or numerical procedures being used. Then the final thermal conductivitiy calculations are made from these data together with the density and heat capacity data of the test material. Thus, this approach is one of determining transient temperature behavior for any nonconstant heat flux and then calculating the result from equation 2. The steady state method, on the other hand, requires a system through which the heat flux is kept as nearly constant as possible. Under this condition, equation 2 reduces to the Laplace of the temperature. Further, if only unidirectional heat flow is considered, the Fourier equation results. From a knowledge of this heat flux, which is determined by one of a number of calorimetric means, and the temperature gradient through the conducting medium, the thermal conductivity can be calculated.

Of the two approaches, the unsteady state one is generally considered the least accurate. It is valued primarily for the arbitrary manner in which it may be executed; the boundary and initial conditions do not have to be known explicitly, or indeed, controlled. This advantage, however, is more than offset by the difficulties in obtaining the required temperature measurements which, of necessity, are a function of time, and all methods of temperature detection are subject to some time lag which, in general, cannot be evaluated with certainty. A further disadvantage is the fact that the density and heat capacity of the conducting medium are required, and these quantities, being calorimetric determinations themselves, are subject to error, which in the final computation of thermal conductivity, add to the overall uncertainty. Hence, even though the experiment is easy to execute, the results are not as precise as might be desired. Sakiadis and Coates[24] made a detailed study of this method and concluded that, at best, results from it are at least 7 per cent uncertain.

Steady state heat transfer, therefore, is most suited for the determination of thermal conductivities. The fact that no heat is accumulated in the steady state systems greatly improves the accuracy of the determination since this eliminates the need for heat capacity and density data. Furthermore, constant temperatures can be measured with more precision than time-dependent ones. Opposed to these advantages, however, are the problems associated with providing a constant heat flux. This requires very careful apparatus design to obtain a constant heat source and heat sink and to insure adequate insulation for controlling the heat flow between them. Thus the problems of steady state determinations are those of temperature control, while the problems of unsteady state experiments are

mainly those of temperature measurement. Past investigators, including Sakiadis and Coates, Bates,[25] Orr and DallaValle,[26] and many others, have studied the advantages and disadvantages of both methods and have concluded that the steady state approach is the more reliable. They have attained accuracies within 3 to 4 per cent. In view of these results, a steady state type apparatus was designed for this project.

2. Apparatus Configuration

A steady state calorimetric device for the measurement of thermal conductivities fundamentally requires a heat source and a heat sink, both at constant temperatures, with the test material thermally connecting the two. A number of apparatus configurations are possible which meet these requirements. These include designs employing concentric spheres and parallel plates. The material of unknown conductivity is contained between the spheres or plates and these, in turn, are maintained at constant but different temperatures. With either of these configurations unidirectional heat transfer is obtained. Multidirectional heat transfer is considerably more difficult to analyze and is experimentally more uncertain; hence, two- or three-dimensional heat transfer is almost never employed. In the present case, some of the systems to be studied were fluids which, of necessity, had to be exposed to temperature gradients. Since this situation can give rise to disruptive convective currents, the design of apparatus was limited by those considerations which minimized convection interferences. For these reasons a parallel plate configuration was chosen.

Convection is governed, both with regard to the configuration and the dimensions of the calorimeter, by the relationship

$$N_{GL}\, N_{PL} = \frac{D^3 \rho^2 g \beta C_p \Delta T}{k \mu} \qquad (29)$$

which is a product of two dimensionless groups, the Grashof number N_{GL} and the Prandtl number N_{PL} where ρ, β, C_p, k, and μ are the fluid density, coefficients of thermal expansion, heat capacity, thermal conductivity, and viscosity, respectively, and g is the gravitational constant, D is the apparatus diameter and ΔT is the temperature across the fluid. The magnitude of the product is a measure of the degree of convection and therefore must be minimized. Of the terms involved, only D and ΔT are subject to change. The linear dimension, D, and the temperature change, ΔT, across this dimension are, however, design variables and are subject to compromise. A reduction of D and ΔT supresses convection effects, and, therefore, suggest that they need to be made as small as possible. Decreasing D is also desirable since this would also reduce the lateral heat losses. On the other hand, D and ΔT should be as large as possible to obtain the greater precision in the measurements. Hence, there actually existed an optimum test medium thickness and an optimum temperature drop.

Of the many configurations for calorimeters that have been considered by other investigators some are broad and thin (disc type), some are exceedingly slender with small cross-sectional areas (capillary type), and others are of moderate proportions having large cross-sectional areas and moderate thicknesses (several centimeters). One of the most satisfactory calorimeters of a moderate type was designed by Bates. It had a cylindrical test section approximately 7.8 cm in diameter and 4.8 cm in depth with the heat flow across the faces of the cylinder. Such dimensions permit accurate

measurement of the thickness of the test medium and provide adequate space for installing temperature sensing devices. The large fluid thickness was justified by the fact that the sides of the calorimeter were guarded to avoid disturbing temperature variations. This control reduces the chance of convection developing by eliminating the occurence of unfavorable temperature distributions. The guard consisted of an annulus of test fluid 38 cm in diameter which was further guarded on its outer periphery by electrical resistance wires. Thus lateral temperature disturbances and asscciated heat losses were practically eliminated. This arrangement provided an essentially constant temperature along any diameter within the test region of the calorimeter.

Later a calorimeter of a somewhat different design was built by Sakiadis and Coates. The heart of this instrument was a cylindrical section 7 inches in diameter that could be adjusted to hold various thicknesses (0 to 2 inches) of the conducting material being tested. Like the Bates design, this apparatus depended on an outer fluid region to guard the smaller region in which the measurements were made. The principal difference in the two designs, other than size, was the method of measuring the heat flow through the apparatus. Bates measured the heat gain of the water circulated through the heat sink whereas Sakiadis and Coates measured the temperature gradient across a comparison block placed between the test medium and the heat sink. The heat flux was calculated from a knowledge of the thermal conductivity of this block and the imposed temperature gradient.

Both these investigators studied the measurement of liquid thermal conductivities very carefully and quantitatively and demonstrated the merits of their techniques. A review of their works showed their devices to be excellent

compromises of the design variables involved. Therefore, these instruments served as practical guides in the designing of an apparatus for this project. Also, in a previous study at Georgia Tech by Orr and DallaValle, an instrument similar to Sakiadis and Coates was used very successfully. Hence, the apparatus developed for this project was similar and included, it is believed, the best features of several previous instruments.

3. Apparatus Construction

Figure 2 shows the principal features of the calorimeter. It was of the steady state, parallel disc type where, as nearly as possible, a constant heat flux was maintained across the test material. The upper plate was maintained at the higher temperature by the circulation of hot water from a constant temperature bath through an attached heating coil. This coil was doubly wound and attached to a copper plate, as shown in Figure 3, so that the heat from the circulating water would be distributed rather evenly over the plate and would create an essentially isothermal surface. Any temperature difference introduced by the heating coil was equalized in the copper plate because the thermal conductivity of copper is so high that it provides essentially an instantaneous distribution of heat. The bottom portion of the hot plate was separated with thin transite insulation into two sections so that the center part of the plate would be guarded against adverse temperature effects at the outer pheriphery of the plate. This division established an intersection, hereafter designated as the test section, and an outersection, the guard section. The champhor at the bottom of the hot plate provided an escape for entrained air beneath the hot plate during assembly of the calorimeter. It was essential that the hot medium contact the hot plate at all points, otherwise intolerable

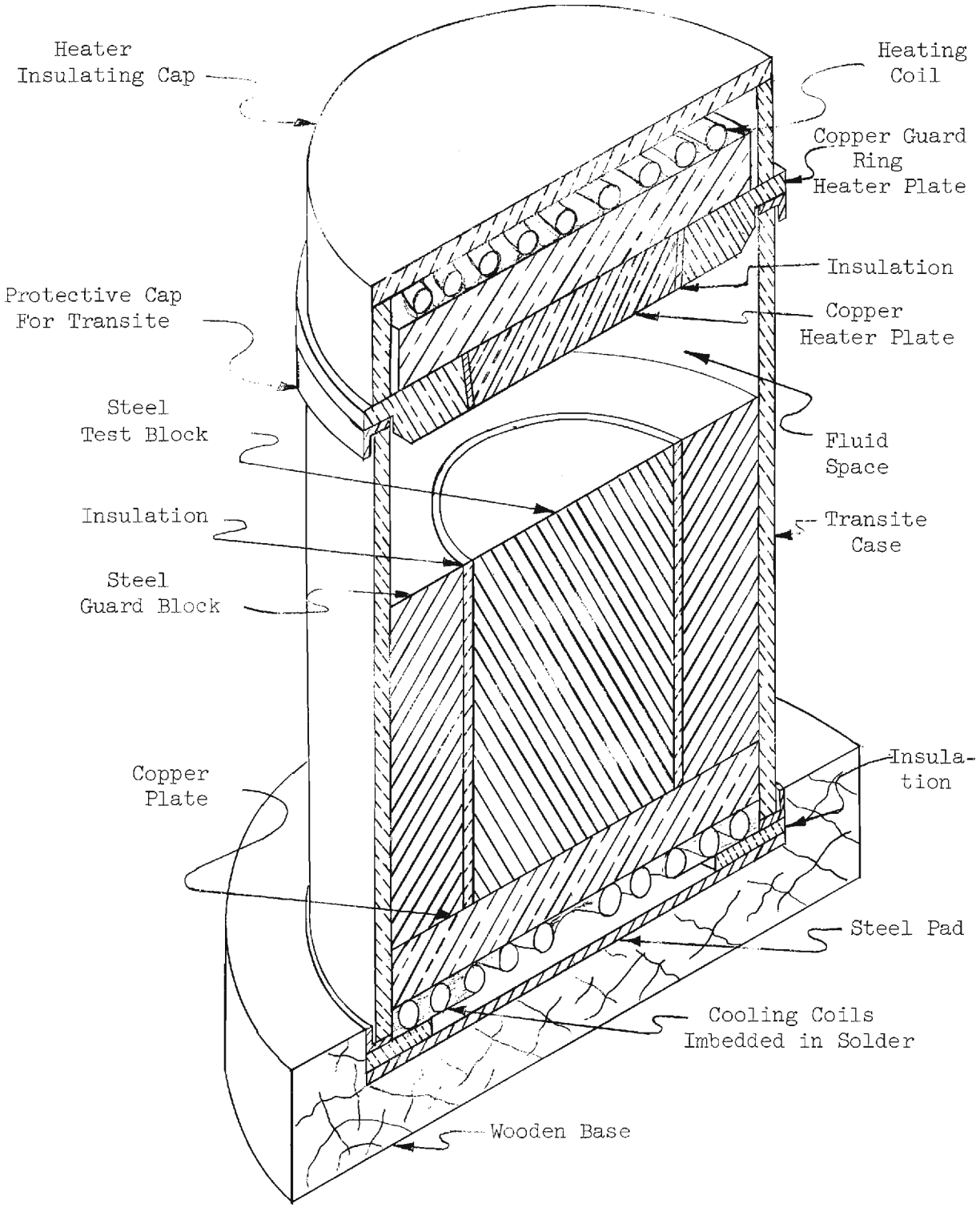

Figure 2. Pictorial Drawing of the Calorimeter.

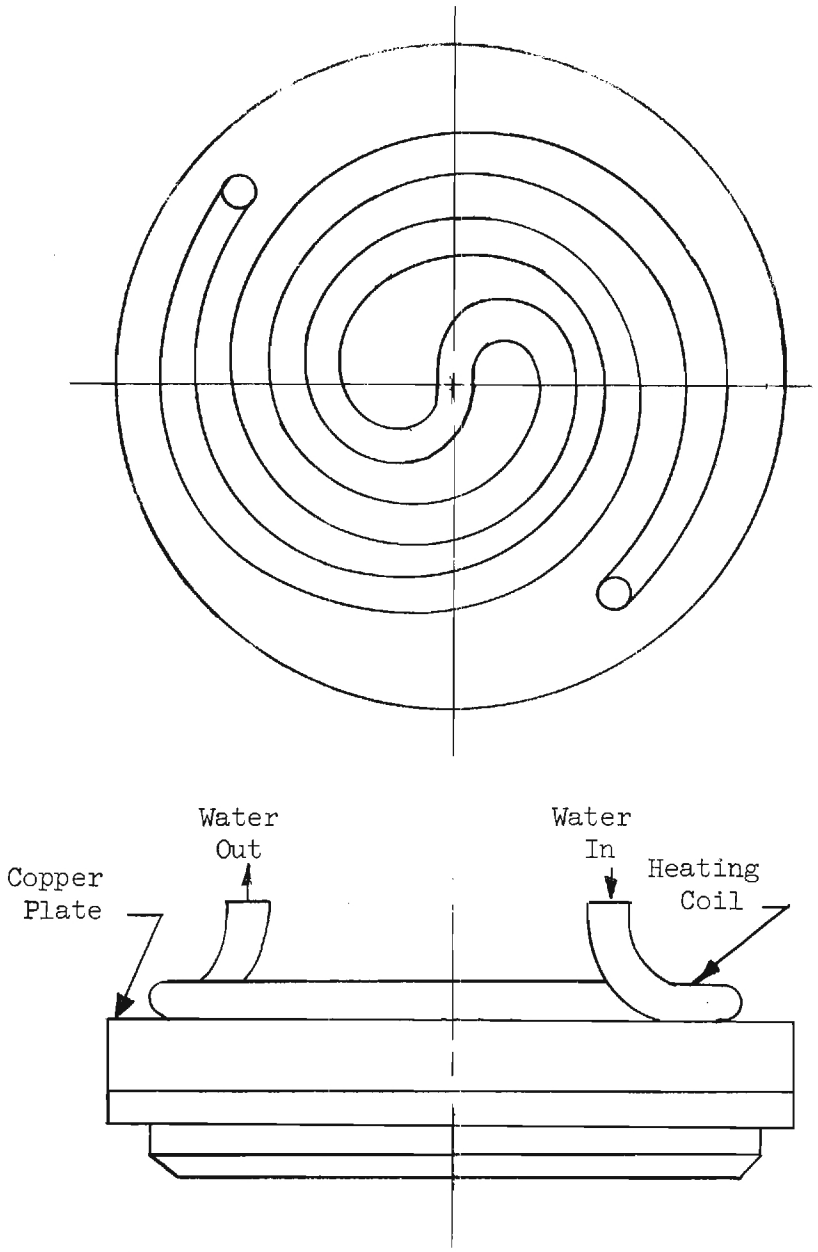

Figure 3. Schematic Drawing of the Dual Wound Heating Coil Attached to a Copper Block. The dual winding distributes the temperature change over the entire surface.

temperature differences would occur in the vicinity of the poor surface contact.

The calorimeter was encased in a transite pipe, the ends of which were capped with steel rings to avoid mechanical damage. Transite was selected for this purpose because its thermal conductivity is lower than metallic construction materials, which makes transite best for low lateral heat losses. Furthermore, neither its strength nor its physical size (thermal expansion) changes appreciably with temperature as do most other construction materials. It is also machinable. The case was 9.75 inches long; it had an inside diameter of 6.09 inches and a wall thickness 0.25 inch.

The test material occupied the region, designated as the fluid space, between the hot plate and the comparison block. This space had a maximum thickness of 2 inches and it could be reduced by inserting machined spacers under the comparison block. There were no physical barriers within this space to establish a guard ring as was done in the hot plate. Such construction would have been detrimental since any difference in the thermal conductivity of the insulator and the surrounding test medium would have produced temperature gradients, and the test medium, being fluid, might have circulated accordingly. Hence, the guard ring effect in the fluid space was obtained by mere extension of the test material beyond the section in which measurements were taken. Since the upper and lower surfaces of the fluid space were maintained, as nearly as possible, isothermal, the inner portion of the test fluid was stabilized by virtue of the inherent density differences imposed by the existing temperature gradient. This stabilizing effect tended to dampen out and to localize the convective effects occuring at the outer wall of the calorimeter.

The comparison block beneath the test medium afforded a measure of the heat flux through the calorimeter, the procedure being to determine the axial temperature gradient through the block and then to calculate the heat flux from equation 1. The thermal conductivity of the block was determined by a calibration which will be explained in a following section. To obtain the best experimental results, the thermal conductivity of this comparison medium should be sufficiently low to provide a measurable temperature drop across a short but also easily definable section. It must also have homogeneous thermal properties; otherwise, heat transfer through the medium is not uniform nor unidirectional as required by the equation. After thorough consideration of these requirements, cold rolled steel was selected as the comparison material. Stainless steel would have been more desirable on account of its slightly lower thermal conductivity, but it could not readily be obtained in the dimensions needed, 6.0 inches in diameter and 6.0 inches in length. This block was sealed to the transite case with "O" rings to prevent fluid leakage. As was done for the hot plate, the comparison block was separated with thin transite insulation, 1/8-inch-thick, into two parts, the guard ring section and the test section.

4. Temperature Control

Basic to the apparatus temperature control was a constant temperature bath which supplied heat to the calorimeter. The electronic control device shown schematically in Figure 4 was constructed for this purpose. In it a thermistor and a variable precision resistor constituted two legs of a Wheatstone bridge. The temperature at which the bridge balanced (the control temperature) was determined by the thermistor and the setting of the variable resistor. When the bridge was in balance the complete circuit

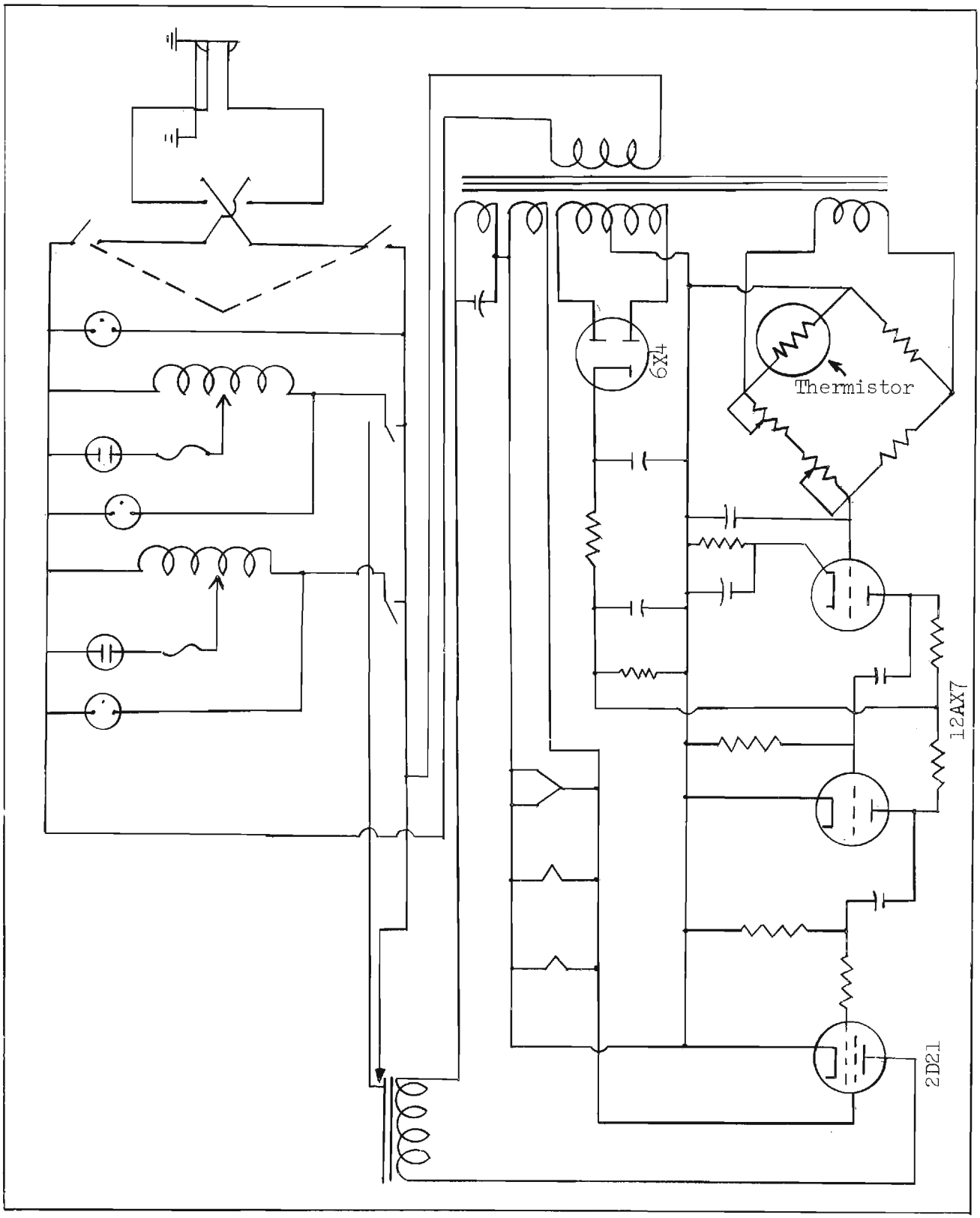

Figure 4. Circuit Diagram of the Hot-Plate Temperature Controller.

was null. When an unbalance occurred, the signal was amplified, and, when it was sufficiently large, a thyratron tube was activated. The pulse caused a relay to close and electric energy to be supplied to a powerstat which, in turn, controlled energy to heaters submersed in the water bath. Energy was added until a resulting temperature increase caused the thermistor to rebalance the bridge, at which time the circuit became null once more and opened the relay. The cycle was repeated when the bath temperature again decreased below the control temperature.

Two powerstats were employed in controlling the electrical energy to the heaters in the hot bath. One was adjusted to supply approximately 80 per cent of the energy required to maintain a constant temperature. This powerstat maintained this setting and was not subject to automatic control. The other powerstat, supplying the remaining energy, was regulated by the controller. This arrangement of furnishing energy to the hot bath smoothed the controlling operation and avoided a completely on-off procedure. By adjustment of the powerstats so that a control cycle occurred approximately every 30 seconds to one minute, it was possible to control the temperature variation within $\pm$ 0.02°C. The ideal, of course, would have been an infinite cycle period. For such a condition, however, there would have been no automatic control. On the other hand, if the cycle time approached zero, the temperature control limits would approach a maximum. Therefore, a compromise between these limits was necessary. By trial and error it was established that one to two cycles per minute was the optimum period. This provided both stable operation and a suitable temperature control limit.

The calorimetric apparatus, being designed for steady state, unidirectional heat transfer, required temperatures and the rate at which heat was

added and removed to remain constant within controllable limits. Thus, strict control of the heat sink for the calorimeter was maintained also. This, however, was readily accomplished by using an ice-water bath for the heat sink. By virtue of the phase relationship between water and ice, the heat sink was, of necessity, at a constant temperature as long as both phases were present, and a second temperature controller was not needed. Agitation of the bath, however, was necessary to maintain the establishment of equilibrium between the ice and water phases. Otherwise, heat absorbed by the bath from the surroundings and from the calorimeter would have shifted the bath equilibrium above that of the ice point.

Even after provision of a constant temperature heat source and heat sink, temperature control must be maintained during the transfer of heat to and from the calorimeter. As previously described, this was accomplished by circulating water from the respective baths through coils attached to the calorimeter end pieces. This required careful control of the water circulation rates to maintain the average water temperature in each coil constant. Since the temperature drop experienced by the circulating water was a function of the residence time in the calorimeter, the average temperature of the coil varied accordingly. Hence, any change in this average temperature was directly related to the constancy of the water circulation rate. Some difficulty was experienced in maintaining adequate control of this process due to surges in line voltages supplying power to the circulating pumps. This, however, was minimized by selecting pumping rates such that the pump performance was not severly affected and the variations were within acceptable limits. Normally the variation in hot and cold temperatures was within $\pm$ 0.05^{o}C, but in extreme cases,

variations of $\pm$ 0.10°C were observed.

The final step in temperature control was provided by adequately insulating the calorimeter. For this purpose, the calorimeter was enclosed in asbestos fiber insulation. Although the test portion of the calorimeter was enclosed completely by a guard ring section, additional protection was necessary. Ambient temperature changes were so large that steady state operation could not be obtained without deep layers of insulation. Further, had not external insulation been provided, the heat exchange through the sides of the calorimeter would have destroyed the unidirectional heat transfer within the calorimeter. Hence, the complete unit was deeply imbedded in asbestos fiber insulation. Figure 5 shows the partially exposed calorimeter. At the time of this photograph cotton waste was used for insulation; this, however was later replaced with asbestos fiber insulation which, it is believed, gave better results. The insulation container was 15 inches in length and width and 20 inches high.

5. Temperature Measurement

The axial temperature gradient through the apparatus and a sufficient number of radial temperature distributions were required to determine the equilibrium conditions in the calorimeter. These temperature measurements were accomplished with a Leeds and Northrup Co., Philadelphia, Pa., precision potentiometer and copper-constantan thermocouples used as temperature-sensing elements. The thermocouples were each calibrated by checking against a National Bureau of Standards certified thermometer at 5 degree intervals over a temperature range from 20° to 75° C and also at the ice point of water. From these data a calibration curve was constructed.

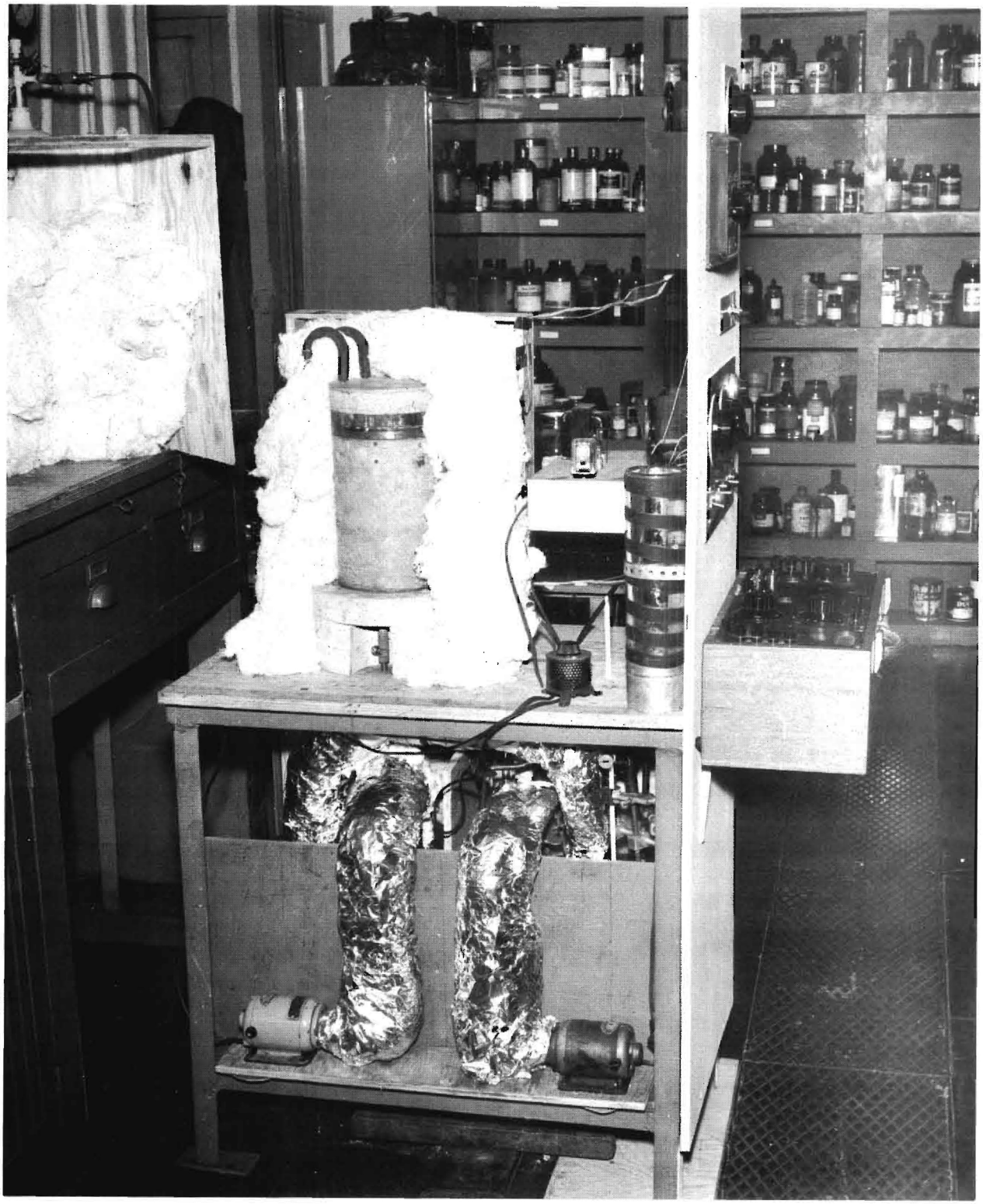

Figure 5. Side View of the Apparatus with a Portion of the Calorimeter Exposed.

It was found to be possible to reproduce temperature readings within $\pm$ 0.02°C. This precision was calculated to afford an overall reproducibility of about 3 per cent in the final results. The calibration was carried out in an agitated water bath supported in an insulated glass jar. Temperature control was accomplished with the instrument which was later used as the heat source temperature controller in the calorimeter itself (see Figure 3). With this system, desired temperatures could be maintained within $\pm$ 0.01°C at temperatures ranging from near room temperature to approximately 50°C. At higher temperatures, heat losses caused temperature variations as high as $\pm$ 0.02°C. By careful setting of the controller these variations could be reduced somewhat, however.

After calibration, the thermocouples were installed in the calorimeter. Installation was begun at the top of the calorimeter where five thermocouples were imbedded near the undersurface of the hot plate. The thermocouples, three of them being situated within the protected center section of the plate and two being in the guard ring, were positioned one at the center and four along a radius 3/4, 1-1/2, 2, and 2-3/4 inches from the center of the plate. The purpose of this layout was to determine the constancy of temperatures over the hot plate. Glyptal, a dielectric varnish of the General Electric Co., Schnectady, N. Y., secured the thermocouples in position with the junctions 1/32 inch from the surface. Glyptal, being hard setting and highly conductive thermally, provided good thermal contact with the hot plate.

Thermocouples in the comparison block have the same radial distributions as those in the hot plate. Figure 6 shows the arrangement of these thermocouples within the steel comparison block. As shown, the

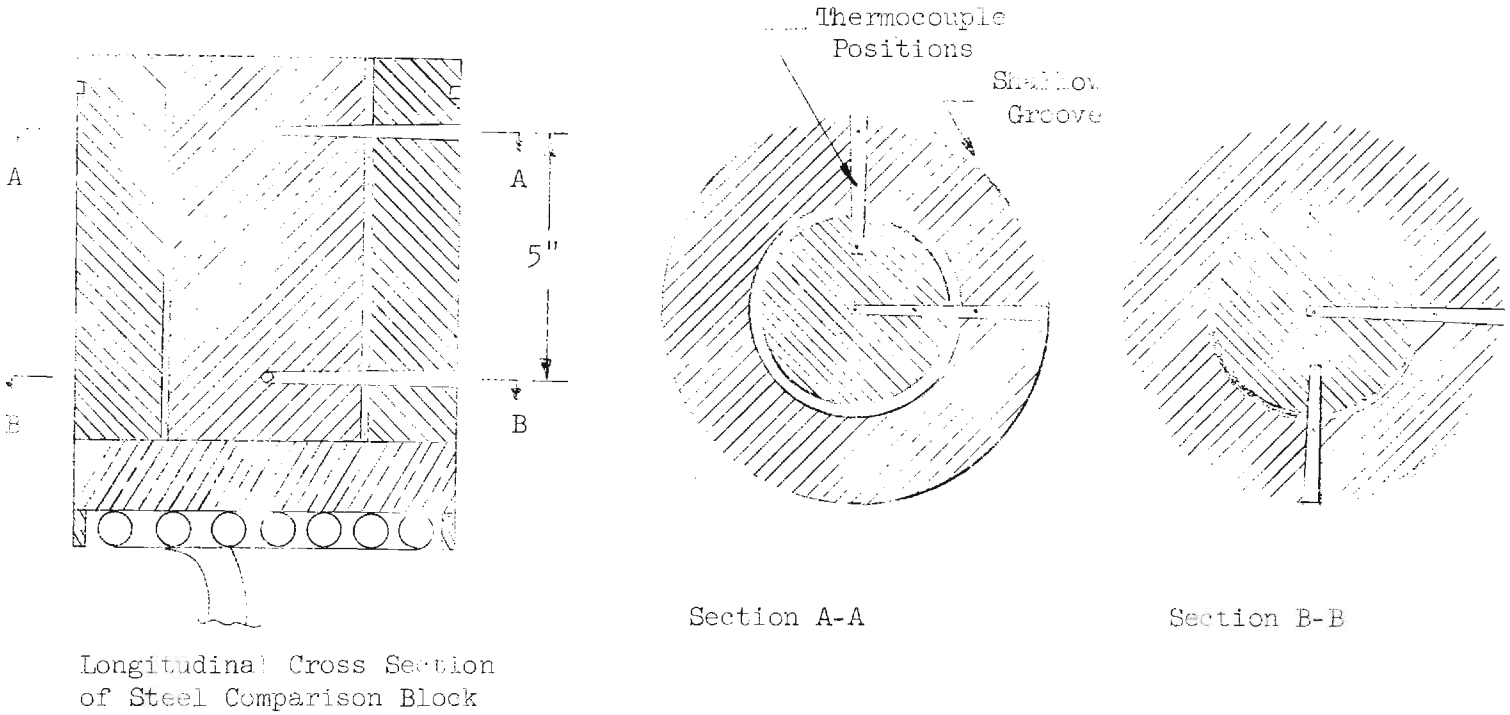

Figure 6. Cross Sections of Steel Comparison Block Showing Placement of Thermocouples.

thermocouples were installed at two levels by use of steel taper pins. A 1/16-inch hole was drilled axially through a No. 5 steel taper pin, and the thermocouples, consisting of 24 B and S wire, were threaded through the pins with the thermocouple junctions terminating inside holes drilled normal to the pin axis. The junctions were located flush with the outer surface of the pin. The pins were then driven into the comparison block. A shallow groove in the side of the comparison block acted as a conduit in which the thermocouple leads were collected and withdrawn from the calorimeter.

Seven thermocouples were positioned along the central axis of the test medium for measuring the temperature gradient there. The thermocouples were mounted in rigid capillary tubes which in turn were supported by a cylindrical plastic sleeve of slightly smaller diameter than that of the calorimeter. Figure 7 presents a drawing of this assembly. The capillary tubes were placed along diameters approximately 1/4 inch apart vertically. Each was displaced angularly relative to the capillary tube immediately above to minimize the thermal interference of neighboring capillary tubes. The thermocouple leads were drawn through the capillary tubes and secured with cement where they emerged from the end of the tubes. There, the leads were gathered to one side of the sleeve and secured to a protective support which led outside the calorimeter.

The use of capillary tubes for mounting the thermocouples in the test medium was a compromise. It would have been much preferred for the thermocouples not to be encased, since the tubes, being of a larger diameter than the thermocouple wire, produced a more far-reaching temperature disruption than the wire alone. Also the increased mass associated

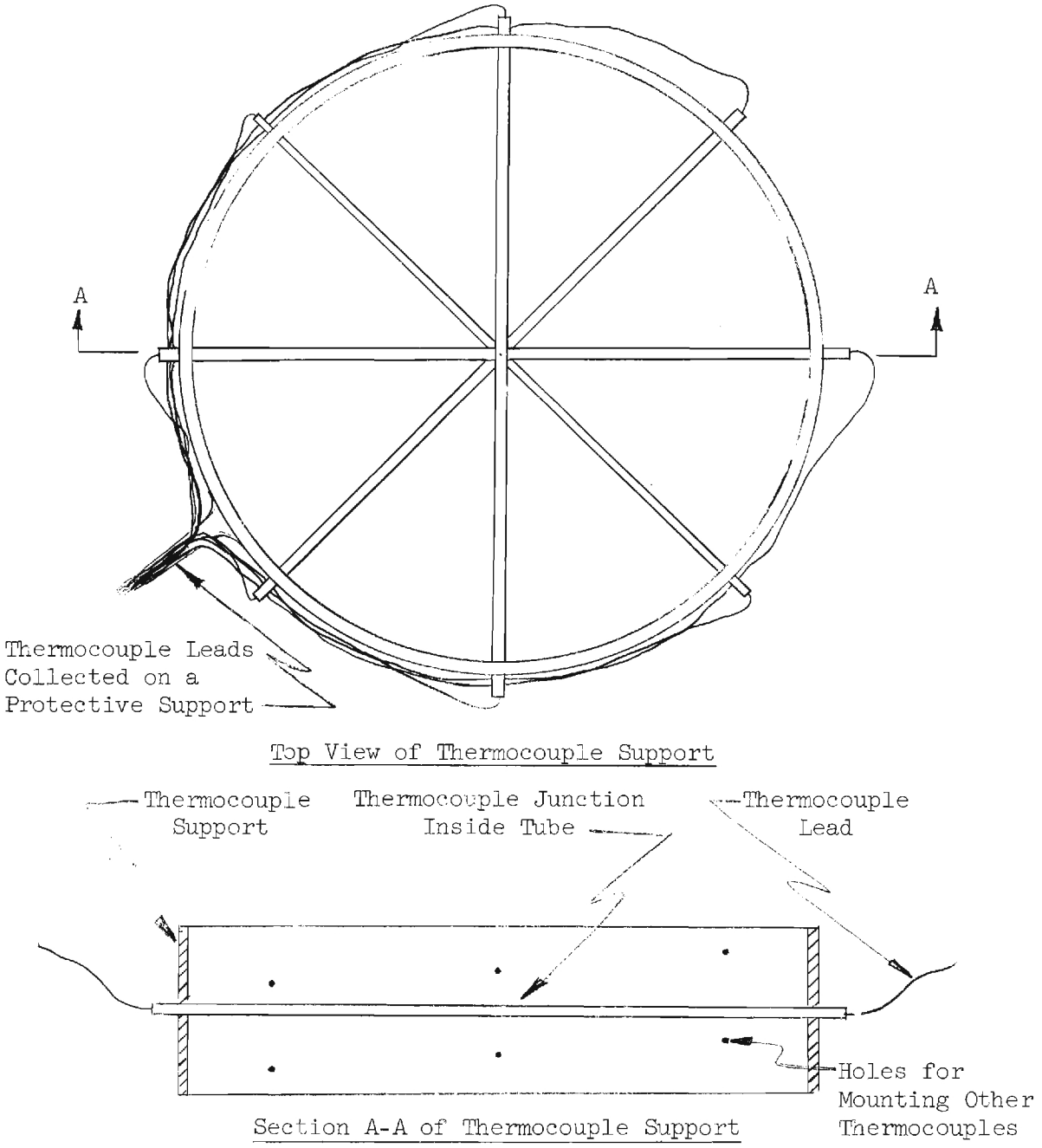

Figure 7. Drawing of the Test Space Thermocouples and Support.

with the thermocouple reduced the sensitivity of the temperature measurements with respect to position. A number of schemes were tried in which the thermocouples were stretched across the fluid space and secured to various spring mechanisms to keep the thermocouples taut. None of these, however, were successful due to damage and displacement incurred during operation. Hence it was necessary to resort to supports for mounting the thermocouples. Although the latter approach was less preferred, results with it appently were quite satisfactory; temperature gradients through the test medium could be determined within ± 2 per cent. To complete the temperature measuring system, all thermocouples were connected through a selector switch to a common cold junction and to the potentiometer.

6. Operation and Calibration

After the calorimeter construction had been completed, a number of preliminary tests were made with pure water both to develop operating procedures and to determine the thermal conductivity to be used for the comparison block. These experiments consisted of bringing the calorimeter to thermal equilibrium with pure water as the fluid transfer medium and then measuring the axial temperature gradients through both the water and the steel comparison block. Temperature determinations were made at periodic intervals to ascertain the stability of the calorimeter operation and to test the reproducibility of the measurements. Water was used as the fluid medium since its thermal conductivity is well established over a considerable temperature range. The data actually used were taken from the Chemical Engineers' Handbook.[27]

Data from two experiments are tabulated in Table XXII.* They

*Experimental data (tables) will be found in the Appendix.

represent a series of temperature gradient determinations in the fluid space, and are included to show the reproducibility of the measurements. Both experiments covered the same temperature range, but interfacial temperature interference between the water and the hot plate produced erronous results in one test, this interference being due to the loss of surface contact by the evaporation of water from the fluid space. In prolonged runs for a given experiment, water had to be added to avoid this adverse effect of evaporation.* If water was not added, temperatures became erratic and operational stability decreased as physical contact was reduced in the interface. In experiment I the temperature difference between the hot plate and the uppermost thermocouple was 11.08°C; in experiment II it was 6.88°C. In both cases the same heat flux prevailed. The difference was due to unequal surface contact with the hot plate.

To study the stability of the heat transfer system, experimental data were taken for approximately 1-1/2 hours of operation after thermal equilibrium had been established. During this time the largest temperature variation was $\pm$ 0.10°C. Such operational stability was considered acceptable for this study. To substantiate this conclusion further, however, the following analysis was made of the experimental data in Table XXII. Since heat transfer through the fluid space is principally by conduction, the Fourier relationship, equation 1, applies. The thermal conductivity of water, being temperature dependent, is described by the expression

*Water was added by means of a glass tube entering the fluid space through the transite wall. The outer portion of the tube was vertical to indicate fluid level inside the calorimeter. The water was charged to the tube with a hypodermic syringe.

$$k = at + b \tag{30}$$

where a and b are constants. Combination and rearrangement of equations 1 and 30 yield:

$$q\, dX = (at + b)\, dt \tag{31}$$

which, upon integration, gives

$$X = \frac{a}{2Q} t^2 + \frac{b}{q} t + C \tag{32}$$

where C is the constant of integration. From equation 32 the temperature distribution through the water can be calculated, provided a, b, and q are known. Values of a and b were taken (reference 31) as 8.03×10^{-3} cal/hr cm $^{\circ}C^2$ and 5.103 cal/hr cm $^{\circ}C$, respectively, and the heat flux q, calculated from the experimental data, was 57.778 cal/hr cm for each experiment. With these values, temperature vs. position distributions were calculated from equation 32 and compared with the experimental data; these results are presented in Table II where it can be seen that calculated and experimental values are in agreement.

Equation 32 shows that distance vs. temperature is a second degree function, and comparison of equations 30 and 32 show that the second degree term is due to the variation of thermal conductivity with temperature. Over the temperature range considered, this variation in the case of water was about 3 per cent and, on a plot of distance vs. temperature, caused a very slight deviation from a straight line. Since this deviation was detectable in the experiments with pure water as the fluid test medium, it was considered that the stability of the calorimeter was such that these

TABLE II

EXPERIMENTAL AND CALCULATED TEMPERATURE DISTRIBUTIONS
FOR PURE WATER AS A HEAT TRANSFER MEDIUM

Experiment I			Experiment II		
	Distance Above Cold Plate			Distance Above Cold Plate	
Temperature (°C)	Measured (Cm)	Calculated[a] (Cm)	Temperature (°C)	Measured (Cm)	Calculated[b] (Cm)
52.20	4.39	4.342	52.70	4.39	4.357
45.40	3.69	3.694	45.60	3.69	3.682
39.70	3.15	3.157	39.55	3.15	3.111
32.70	2.51	2.503	33.00	2.51	2.500
26.00	1.87	1.899	26.15	1.87	1.849
18.40	1.19	1.189	18.75	1.19	1.190
11.55	0.57	0.570	11.90	0.57	0.570

[a] Calculated from Equation 32: $X = (6.954 \times 10^{-5})\ T^2 + (8.833 \times 10^{-2})\ T - 0.4595$

[b] Calculated from Equation 32: $X = (6.954 \times 10^{-5})\ T^2 + (8.833 \times 10^{-2})\ T - 0.4909$

measurements had a precision of approximately 3 per cent. Of course, the overall error for the calorimeter was more than this due to the experimental error introduced by use of the comparison block.

In addition to the investigation of the stability of the calorimeter, experiments with pure water were used to calibrate the thermal conductivity of the comparison block. From knowledge of the temperature gradient in both the water and in the comparison block, the thermal conductivity of the comparison block could be calculated from the equation

$$k_b = k_w \frac{(dt/dx)_w}{(dt/dx)_b} \tag{33}$$

From such a series of experiments, k_b was found to be 19.3 BTU/hr ft ^{o}F. It should be noted that, since the thermal conductivity of the water was temperature dependent, k_w and $(dt/dx)_w$ had to be evaluated at the same temperature to achieve the correct result. Once this constant was established, however, equation 33 could be rearranged and used for determining the thermal conductivities of materials occupying the fluid space. It becomes

$$k_m = 19.3 \frac{(dt/dx)_b}{(dt/dx)_m} \tag{34}$$

where k_m and $(dt/dx)_m$ refer to the thermal conductivity and the thermal gradient through the material in the test space of the calorimeter and the dimensional units for k_m is BTU/hr ft ^{o}F. Thus, a determination of the thermal gradients through a material of unknown conductivity and the corresponding thermal gradient through the comparison block was sufficient to calculate the unknown's thermal conductivity.

B. Experimental Data for Suspensions

1. Glass Beads-Water (Gelled) Suspensions

The first portion of this project involved a study of the thermal conductivity of two-phase systems with particular reference to the characterization of the dispersed phase and particulate properties such as shape, size, and specific surface area. The study was initiated with glass beads (Superbrite glass beads, Minnesota Mining and Manufacturing Company, Minneapolis, Minn.) as the dispersed phase. This material was chosen for initial study because of the size uniformity and the spherical nature of the beads.

It was necessary first to establish a technique for preparing stable, uniform glass beads-water suspensions, however. Of several techniques tried, the following was adopted: A 3-1/2-weight-per-cent aqueous solution of agar was prepared. This solution was then heated between 80° and 90° F to effect complete solution of the agar. The desired volume of glass beads was then added slowly to the agar solution which was vigorously agitated to disperse the beads. The suspension was next cooled slowly toward the agar gelling temperature. Meanwhile, having been transferred to a stoppered Erlenmeyer flask, the suspension was shaken gently to avoid settling of the beads. The flask was also periodically inverted to reverse the settling direction. As the gelling temperature was approached the suspension was agitated less and less to avoid entrainment of air bubbles. When the gel formed sufficiently for the beads to remain suspended without agitation, the suspension was quickly transferred to the calorimeter.

Not every attempt resulted in an acceptable suspension. Close observation and careful timing were essential as the gelling temperature of the agar was approached. Agitation at this point had to be reduced to a

minimum, for air bubbles were easily entrained, and, once captured, they could not escape before the gel set completely. Also there was a very definite time at which the suspension had to be transferred to the calorimeter. If the suspension was transferred prematurely, the beads settled either partly or completely before sufficient gelling occurred. If the transfer was too late, the gel became too thick to pour into the calorimeter. It was also important that agitation immediately cease when gelling commenced, for further agitation served only to break the gel and to allow the beads to settle.

Using the outlined technique for preparing gels, a series of experiments was performed with glass bead suspensions. The experimental data for these tests are presented in Table XXIII in the Appendix. Data are included for glass bead concentrations of 0, 25, 37, 50, and 71 weight per cent, the beads being between 75 and 125 μ in diameter. The calculated thermal conductivity results are presented in Table II. To eliminate the effect of the gelling agent on the thermal properties of the continuous phase the results were evaluated relative to the gel rather than water. The gel apparently lowered the conductivity of the water by about 3 per cent.

TABLE III

CALCULATED RESULTS FOR GLASS BEADS-WATER (GELLED) SUSPENSIONS

Glass Beads Concentration		
Weight Fraction	Volume Fraction	Suspension Thermal Conductivity (BTU/Hr Ft °F)
0.00	0.00	0.355
25	0.12	0.384
37	0.19	0.356
50	0.29	0.371
71	0.50	0.394

2. Zinc-Grease Suspensions

Following the study of glass beads-water (gelled) suspensions, attention was turned to an investigation of zinc particles suspended in automobile lubricant (Marfak No. 1 lubrication grease, Texaco Oil Company.) The selection of this system was guided both by the objective of the project and by the results for the glass beads-water suspensions. The lubricant was substituted for water as the continuous phase since its viscosity was such that no gelling agents were required. Thus the procedure for preparing suspensions was immensely simplified; it amounted merely to mixing together the desired amounts of each phase until the mixture was of a uniform consistency. This approach was much more practical since considerable difficulty was experienced in maintaining uniformity between the various gel preparations. Also, the thermal conductivity of the automobile lubricant remained fixed for any series of experiments whereas the properties of a gel varied with each preparation. Zinc was selected as the dispersed phase since its extremely high thermal conductivity (compared with grease) would produce a marked dependence of the suspension thermal conductivity on the dispersed phase composition and thus make the experimental results more easily analyzed. For the lower concentrations especially, little could be learned from the glass beads-water measurement since the variation of suspension thermal conductivity was less than the experimental error.

Zinc paint pigment was the source of the zinc particles. Two zinc samples, designated as zinc A and zinc B, having different particle size distributions and, consequently, different surface areas, were employed. Quantitative measurements of the particle sizes showed that zinc A and zinc B had mass mean particle diameters of 80 and 60 μ with standard derivations

of 1.6 and 1.4, respectively. The particles of both materials were irregularly shaped. Surface area determinations by the BET method indicated that zinc A had a surface area of 0.17 m^2/gm while zinc B had 0.19 m^2/gm. Thermal conductivity measurements were made for suspensions of these powders ranging from zero (pure grease) to 90 per cent zinc by weight. The experimental data are tabulated in Tables XXIV and XXV, while the calculated results are given in Table IV.

Additional experiments were made with a zinc B suspension containing a surfactant. This study was designed to test whether such additions to the fluid phase would alter interfacial surface properties and thereby change the heat transfer mechanism. The experimental procedure was to prepare a series of zinc B suspensions and make experimental determinations on each suspension both with and without surfactant being added. Armeen-2S, a mixture of unsaturated primary fatty amines, produced by Armour and Company, Chicago, Illinois, was employed as the surfactant. The experimental data for these experiments are presented in Tables XXVI and XXVII, and the calculated results are shown in Table V. As shown, data were collected for the surfactant free suspensions with zinc compositions ranging from zero to 80 weight per cent zinc. Of these determinations, comparative experiments were made with surfactant being added to the 0, 60, 70, and 80 per cent zinc suspensions. For the latter experiments the grease phase contained one per cent Armeen-2S by weight.

3. Aluminum-Grease Suspensions

Aluminum in grease suspensions were also investigated since aluminum powder could be obtained with the particles widely varying in

TABLE IV

CALCULATED RESULTS FOR ZINC-GREASE SUSPENSIONS

Zinc Composition		Suspension Thermal Conductivity (BTU/Hr Ft °F)	
Weight Fraction	Volume Fraction	Zinc A	Zinc B
0.00	0.00	0.170	0.170
0.20	0.03	0.190	--
0.40	0.08	0.204	--
0.50	0.11	--	0.233
0.60	0.16	0.220	0.237
0.70	0.22	0.260	0.260
0.75	0.27	0.302	--
0.80	0.33	0.332	0.320
0.85	0.41	0.372	--
0.90	0.53	0.497	0.478

TABLE V

CALCULATED RESULTS FOR ZINC-GREASE SUSPENSIONS
IN THE STUDY OF SURFACTANT EFFECTS

Zinc Composition		Suspension Thermal Conductivity (BTU/Hr Ft °F)	
Weight Fraction	Volume Fraction	Zinc B	Zinc B with Surfactant*
0.00	0.00	0.163	0.167
0.20	0.03	0.171	--
0.40	0.08	0.186	--
0.60	0.16	0.220	0.226
0.70	0.22	0.243	0.231
0.80	0.33	0.322	0.312

*Armeen 2S amounting to 1 per cent of the weight of the grease.

physical shape. As in the case of zinc, it was anticipated that the high thermal conductivity of aluminum was so large that any effects of particulate properties would be magnified and thus more easily evaluated. Three geometrical shapes, spherical, irregular and platelet, were utilized to determine the effect of particulate shape on suspension thermal conductivity. Further, spherical powders were separated into three distinct particle size distributions to study the effect of particle size. These spherical powders, hereafter referred to as aluminum A, aluminum B, and aluminum C, had mass mean diameters of 33, 40, and 53 μ with standard deviations of 2.5, 1.8, and 1.5 and surface areas of 1.3, 1.0, and 0.6 m^2/gm, respectively. The irregular aluminum powder had a mass mean size of 40 μ, a standard derivation of approximately 2.0 and a surface area of 0.6 m^2/gm. A detailed analysis of the flake aluminum was not made; the surface area, however, was determined to be 5.0 m^2/gm and the average flake diameter was approximately 40 μ.

The experimental data for the aluminum-grease experiments are presented in Tables XXVIII through XXXII. The aluminum composition ranged from zero (pure grease) to between 50 and 60 per cent aluminum by weight. The calculated results are tabulated in Tables VI and VII. It should be noted that the data for the flake aluminum, Table VII, indicate a dependence of thermal conductivity on suspension temperature. Otherwise the data are similar to those for glass beads-water and zinc-grease suspensions.

C. Experimental Data for Emulsions

Four systems were employed in the study of emulsion thermal conductivity. These systems, composed of water and one of the organic liquids,

TABLE VI

CALCULATED RESULTS FOR IRREGULAR ALUMINUM-GREASE SUSPENSIONS
AND SPHERICAL ALUMINUM-GREASE SUSPENSIONS

Aluminum Composition		Thermal Conductivity (BTU/Hr Ft °F)			
Weight Fraction	Volume Fraction	Irregular Aluminum	Aluminum A	Aluminum B	Aluminum C
0.00	0.000	0.164	0.151	0.152	0.152
0.20	0.074	0.185	0.173	0.167	0.170
0.30	0.120	0.191*	0.180	0.174	0.179
0.40	0.175	0.202	0.197	0.198*	0.192
0.50	0.242	0.248*	0.218	0.218	0.210
0.60	0.323	0.339	0.259	0.246*	0.237*

*These values were obtained from a smoothed curve of the experimental data.

TABLE VII

CALCULATED RESULTS FOR FLAKE ALUMINUM-IN-GREASE SUSPENSIONS

Temperature (°C)	Suspension Thermal Conductivity (BTU/Hr Ft °F) at Weight Per Cent Compositions of				
	0%	20%	30%	40%	50%
50	0.159	0.467	1.290	1.458	0.307
40	0.159	0.332	0.594	0.693	0.599
30	0.159	0.311	0.378	0.435	0.751
25	0.159	0.305	0.354	0.370	0.778
20	0.159	0.302	0.350	0.333	0.798

carbon tetrachloride, hexane, diethylbenzene, or turpentine, were selected on the basis of availability of components and the ability to prepare stable emulsion from them over a wide composition range. Emulsification was accomplished with a hand homogenizer, the procedure being to mix partially the two phases by shaking and then to process the mixture in the homogenizer a sufficient number of times to obtain the emulsified state. A small amount of surfactant dissolved in the continuous phase stabilized the emulsion and thus prevented coagulation of the dispersed phase. The selection of the proper surfactant had to be determined by trial and error, and, hence, was the time-consuming part of developing the emulsification procedure. This was further complicated by the fact that more than one surfactant was sometimes required to cover the range of compositions desired. The carbon tetrachloride-water emulsion was a system of the latter type. For very low carbon tetrachloride concentrations, agar was used as a surfactant while increasingly higher compositions required Tween 61 and finally Tween 20.

Tween 61 and Tween 20 are products of the Atlas Powder Company, Wilmington, Del., and are sodium salts of organic acids. The hexane-water and the diethylbenzene-water emulsions required only Tween 20 for stabilization.

Experimental data for the emulsion conductivities are presented in Tables XXXIII through XXXVI, while the calculated results are tabulated in Tables VIII through XI. As shown, compositions by weight up to 70 per cent organic phase were investigated for the carbon tetrachloride-water and hexane-water emulsions and up to 80 weight per cent for the turpentine-water system. The diethylbenzene-water emulsions, however, could not be investigated above compostions of 60 weight per cent organic, since higher compositions of the diethylbenzene attacked the thermocouple supporting structure of the calorimeter.

TABLE VIII

CALCULATED RESULTS FOR CARBON TETRACHLORIDE-AND-WATER EMULSIONS

Carbon Tetrachloride Composition		
Weight Fraction	Weight Fraction	Thermal Conductivity (BTU/Hr Ft ^{o}F)
0.00	0.00	0.328[a]
0.20	0.14	0.290[a]
0.40	0.30	0.278[a]
0.60	0.49	0.195[b]
0.70	0.59	0.204[c]

(a) Emulsifying agent 2 per cent agar; (b) 0.5 per cent Tween 61; (c) 1.0 per cent Tween 20. Percentages are of total emulsion weight.

TABLE IX

CALCULATED RESULTS FOR HEXANE-AND-WATER EMULSIONS

Hexane Composition		
Weight Fraction	Volume Fraction	Thermal Conductivity (BTU/Hr Ft ^{o}F)
0.00	0.00	0.352
0.20	0.28	0.281[a]
0.30	0.39	0.255[b]
0.40	0.50	0.214[b]
0.50	0.60	0.213[b]
0.60	0.70	0.165[b]
0.70	0.78	0.147[c]

(a) Emulsifying agent 1.0 per cent Tween 61; (b) 2.0 per cent Tween 61; (c) 3.0 per cent Tween 61. Percentages are of total emulsion weight.

TABLE X

CALCULATED RESULTS FOR DIETHYLBENZENE-AND-WATER EMULSIONS

Diethylbenzene Composition		
Weight Fraction	Volume Fraction	Thermal Conductivity (BTU/Hr Ft °F)
0.00	0.00	0.352
0.20	0.23	0.305[a]
0.40	0.44	0.259[a]
0.60	0.64	0.217[b]

(a) Emulsifying agent 1.0 per cent Tween 61; (b) 1.5 per cent Tween 61. Percentages are of total emulsion weight.

TABLE XI

CALCULATED RESULTS FOR TURPENTINE-AND-WATER EMULSIONS*

Turpentine Composition		
Weight Fraction	Volume Fraction	Thermal Conductivity (BTU/Hr Ft °F)
0.00	0.00	0.352
0.20	0.22	0.340
0.40	0.43	0.268
0.60	0.63	0.200
0.80	0.82	0.164

*Emulsifying agent Tween 20, 1.0 per cent of total emulsion by weight.

D. Experimental Data for Powder Beds

The third phase of this project was an investigation of solid-gas systems, more commonly referred to as powder beds. The factors involved in the thermal conductivity of such systems are the size, shape, and thermal properties of the particle material and the properties of the gas filling the intervening spaces among the particles. The effect of these variables was studied by making thermal conductivity determinations on several glass beads-gas systems in which the glass beads had average diameters of 36, 290, 350, and 750 μ. This series of experiments was performed with air, helium, and methane as the intervening gas. Experimental data for these measurements are tabulated in Table XXXVII and the calculated thermal conductivities are presented in Table XII. The method for measuring the temperature gradient across the powder bed was necessarily different from that used with suspensions and emulsions. In the case of suspensions and emulsions, thermocouples were arranged along the central axis of the fluid space, whereas for the powder beds the temperature drop was determined only by a measurement of the temperature of the adjoining hot and cold surfaces. Thermocouples could not be positioned in the powder bed without disturbing their location when the bed was compressed during apparatus assembly. The separation between the hot and cold plates was reduced from 2 inches to 3/4 inch.

TABLE XII

CALCULATED RESULTS FOR GAS-GLASS BEADS SYSTEMS

System	Thermoconductivity of Gas-Glass Beads Bed (BTU/Hr Ft ^{o}F)
Air-glass beads 36μ average diameter	0.106
Air-glass beads 290μ average diameter	0.121
Air-glass beads 340μ average diameter	0.125
Air-glass beads 750μ average diameter	0.128
Helium-glass beads 750μ average diameter	0.130
Natural gas-glass beads 36μ average diameter	0.115
Natural gas-glass beads 290μ average diameter	0.137
Natural gas-glass beads 340μ average diameter	0.146
Natural gas-glass beads 750μ average diameter	0.148

V. DISCUSSION OF RESULTS

A. Suspensions

As the first step in analyzing for the dependence of suspension thermal conductivity on such variables as shape, size, and surface properties of the dispersed phase, as well as the properties of the pure components, the experimentally determined thermal conductivities of zinc-grease and aluminum-grease suspensions were plotted as a function of solid phase composition. For the case of zinc, the suspension thermal conductivities at corresponding solids concentration were very nearly identical for both types of particles investigated. As noted in the presentation of the experimental data, the zinc particles were irregular in shape and had specific surface areas of 0.19 and 0.17 m^2/gm and mean particle diameters of 80 and 60 μ, respectively. The experimental data for these powders, therefore, indicated that suspension thermal conductivity is a weak function of particle size and particle surface area, at least in this size range. There was a 25 per cent difference in particle size and a 10 per cent difference in surface area, yet both curves were the same within experimental error. The same conclusion can be drawn from the data on aluminum-grease suspensions. It is seen that the thermal conductivities of spherical aluminum suspensions were essentially independent of the particle size of the suspended phase. The aluminum powders (samples A, B, and C) used in these experiments had particle sizes with mass mean diameters of 33, 40, and 53 μ, respectively. Thus, an almost twofold change in particle size resulted in negligible change in suspension thermal conductivity. It should be noted that the same result was obtained regardless of particle shape; the zinc particles were irregular and the aluminum particles were spherical.

The data also show that the thermal conductivities of suspensions having corresponding particle concentrations are considerably higher in the case of irregular aluminum suspension than they are for spherical aluminum suspensions. Because the irregular aluminum powder had an average particle size of 40μ and a standard deviation of approximately 2.0, this powder was almost identical to the spherical aluminum samples except for particle shape. Hence the difference in the experimental results showed that the suspension thermal conductivity was rather strongly dependent on particle shape.

It should be noted why the results for the flake aluminum suspensions have so far been omitted from the discussion of particle shape effects. Unfortunately, the results were not directly interpretable. As shown in Figure 8 the thermal conductivities of these suspensions seem to be a function of both temperature and aluminum composition, a fact which theoretically should not have been possible. The thermal conductivity of neither aluminum nor automobile grease change radically with temperature, hence the thermal conductivity of the mixture should be nearly temperature independent. The dependence of thermal conductivity on the suspension's temperature was at first thought to be due to the chemical reaction of contaminants, perhaps associated with the aluminum. Hence, to check this hypothesis a second series of experiments was performed with an aluminum sample which was supposedly chemically pure. The same behavior was again obtained. Then, since the temperature effect still had not been removed, efforts were made to develop a calculation to correct for the generation or absorption of heat. Several calculations were carried out both for cases of constant heat generation (or absorption) and for cases of heat generation varying arbitrarily with temperature. None of these

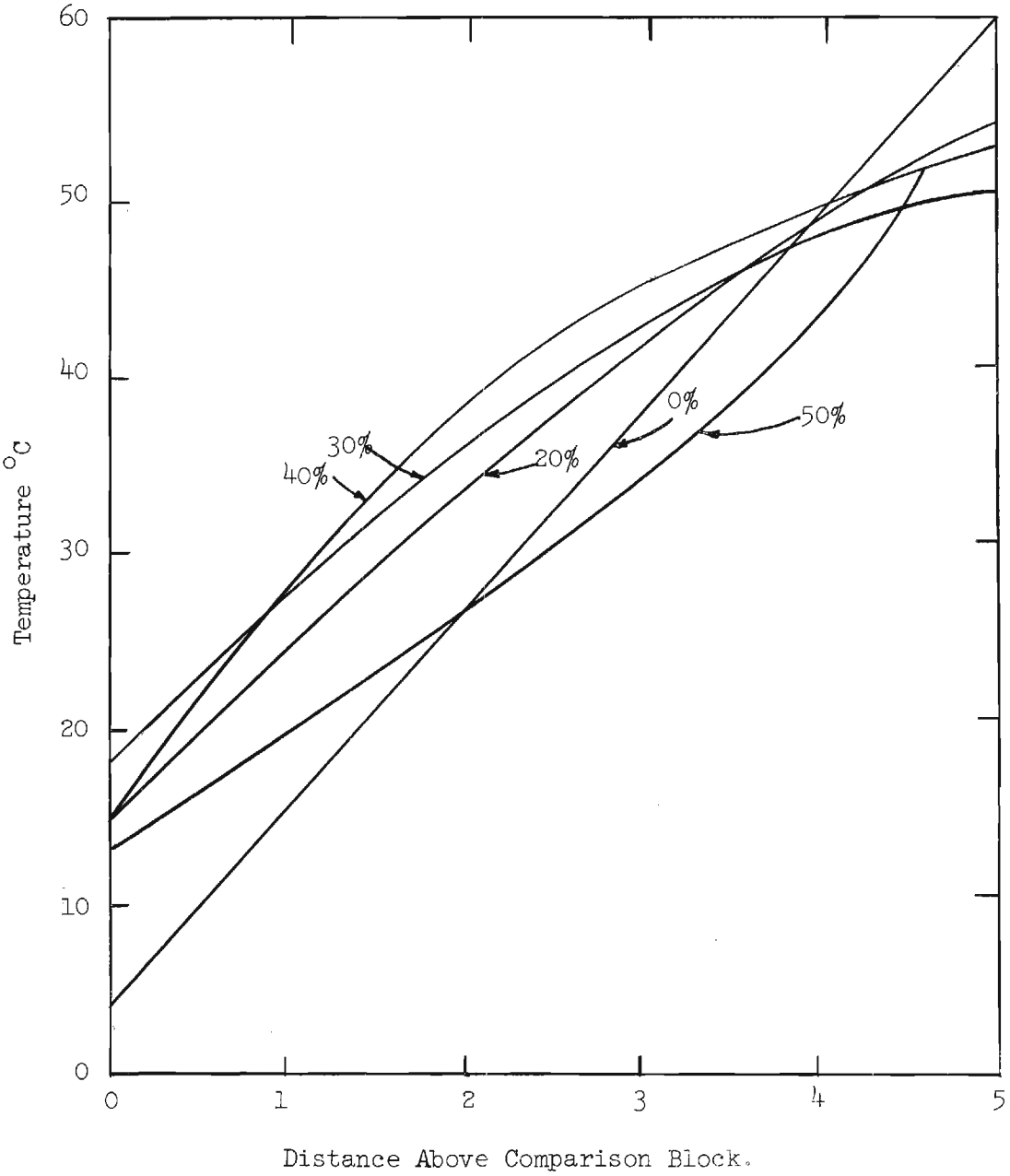

Figure 8. Temperature Profiles for Several Compositions of Flake Aluminum in Grease.

attempts was successful. The results for the flake aluminum have not been used in the final analysis of the experimental data for suspensions.

The effect of adding surfactants to the fluid phase was also determined directly from the experimental data. As shown in Table V, the conductivities for zinc B-grease suspensions were not significantly different when the surfactant, Armeen-2S, was added, even at very high concentrations. This result should have significance for other systems since this system, having a large (over 100) ratio of the dispersed phase thermal conductivity to that of the fluid phase, should be highly sensitive to any changes produced in the heat conduction mechanism. For systems where this same ratio is low, a change in surface properties should be even less effective. That this is true is demonstrated by the fact that thermal conductivity computations are relatively insensitive to particulate properties for low ratios of dispersed phase thermal conductivity to that of the continuous phase. Computations that show this are discussed in a later section of this report. The change in thermal conductivity may, of course, be a function of the surfactant employed; that the Armeen-2S had an influence, however, was apparent from the substantial reduction in suspension viscosity when Armeen 2S was added.

Besides the comparison of the different sets of experimental data, an analysis was made of these data with respect to various analytical expressions. Tables XIII, XIV, and XV present these calculations. As may be readily seen, calculated values were predominately higher than the experimental results. With the exceptions of equations 9, 12, and 15a, which gave extremely high values, the analytical results differed from the experimental values by 50 per cent at low solids concentration and by

TABLE XIII

COMPARISON OF EXPERIMENTAL RESULTS AND ANALYTICAL COMPUTATIONS FOR GLASS BEADS-GEL SUSPENSIONS*

Data Source	Thermal Conductivity (BTU/Hr Ft ^{o}F) for Weight Fractions and, in Parentheses, Corresponding Volume Fractions of				
	0.00 (0.00)	0.25 (0.12)	0.37 (0.19)	0.50 (0.29)	0.70 (0.50)
Experimental	0.355	0.384	0.356	0.371	0.394
Calculated, eq. No. 3	0.360	0.394	0.416	0.446	0.518
Calculated, eq. No. 7	0.360	0.394	0.416	0.448	0.522
Calculated, eq. No. 9	0.360	0.395	0.415	0.449	0.523
Calculated, eq. No. 10	0.360	0.394	0.415	0.447	0.520
Calculated, eq. No. 11	0.360	0.396	0.419	0.456	0.555
Calculated, eq. No. 12	0.360	0.397	0.421	0.459	0.560
Calculated, eq. No. 13	0.360	0.392	0.412	0.447	0.536
Calculated, eq. No. 14	0.360	0.398	0.422	0.458	0.541
Calculated, eq. No. 15a	0.360	0.404	0.430	0.467	0.545
Calculated, eq. No. 15b	0.360	0.383	0.398	0.423	0.482

*Equation No. 18 not applicable in this system.

TABLE XIV

COMPARISON OF EXPERIMENTAL RESULTS AND ANALYTICAL COMPUTATIONS FOR ZINC-GREASE SUSPENSIONS

Data Source	Thermal Conductivity (BTU/Hr Ft °F) for Weight Fractions and, in Parentheses, Corresponding Volume Fractions of					
	0.00 (0.00)	0.20 (0.03)	0.40 (0.08)	0.60 (0.16)	0.70 (0.22)	0.80 (0.33)
Experimental	0.163	0.171	0.186	0.220	0.243	0.322
Calculated, eq. No. 3	0.170	0.186	0.214	0.268	0.314	0.431
Calculated, eq. No. 7	0.170	0.185	0.218	0.283	0.353	0.556
Calculated, eq. No. 9	0.170	0.185	0.218	0.283	0.353	0.556
Calculated, eq. No. 10	0.170	0.186	0.214	0.267	0.314	0.431
Calculated, eq. No. 11	0.170	0.186	0.216	0.275	0.330	0.467
Calculated, eq. No. 12	0.170	1.47	6.85	23.2	49.8	125.
Calculated, eq. No. 13	0.170	0.181	0.200	0.237	0.271	0.352
Calculated, eq. No. 14	0.170	0.186	0.217	0.272	0.324	0.447
Calculated, eq. No. 15a	0.170	2.160	5.316	10.464	14.323	21.400
Calculated, eq. No. 15b	0.170	0.175	0.185	0.202	0.218	0.253
Calculated, eq. No. 18	0.170	0.180	0.196	0.239	0.276	0.407

TABLE XV

COMPARISON OF EXPERIMENTAL RESULTS AND ANALYTICAL COMPUTATIONS FOR ALUMINUM-GREASE SUSPENSIONS

Data Source	Thermal Conductivity (BTU/Hr Ft °F) for Weight Fractions and, in Parentheses, Corresponding Volume Fractions of							
	0.00 (0.00)	0.20 (0.07)	0.30 (0.12)	0.40 (0.18)	0.50 (0.24)	0.60 (0.32)	0.70 (0.43)	0.80 (0,56)
Experimental								
1. Irregular Al particles	0.164	0.185	0.191	0.202	0.248	0.339	0.416	0.834
2. Spherical Al A	0.151	0.173	0.180	0.197	0.218	0.259	--	--
3. Spherical Al B	0.152	0.167	0.174	0.198	0.218	0.246	--	--
4. Spherical Al C	0.152	0.170	0.179	0.192	0.210	0.237	--	--
Calculated, eq. No. 3	0.170	0.210	0.238	0.278	0.333	0.412	0.545	0.814
Calculated, eq. No. 7	0.170	0.212	0.254	0.300	0.390	0.535	0.880	1.880
Calculated, eq. No. 9	0.170	0.212	0.254	0.300	0.390	0.535	0.880	1.880
Calculated, eq. No. 10	0.170	0.210	0.238	0.278	0.335	0.424	0.604	0.141
Calculated, eq. No. 11	0.170	0.212	0.242	0.288	0.348	0.459	0.647	1.06
Calculated, eq. No. 12	0.170	16.8	43.0	95.5	178.0	384.0	770.0	1690.0
Calculated, eq. No. 13	0.170	0.200	0.217	0.245	0.290	0.347	0.454	0.685
Calculated, eq. No. 14	0.170	0.213	0.242	0.287	0.337	0.437	0.598	0.957
Calculated, eq. No. 15a	0.170	8.889	14.310	20.790	28.685	38.229	50.248	66.155
Calculated, eq. No. 15b	0.170	0.184	0.193	0.206	0.224	0.251	0.295	0.386
Calculated, eq. No. 18	0.170	0.203	0.232	0.280	0.364	0.503	0.823	2.040

100 per cent at high solids concentration. For the zinc and aluminum suspensions in grease, equation 13 gave the best overall results. Values calculated from this equation differed from the experimental data by a maximum of 25 per cent. The experimental results for the spherical aluminum suspensions, however, were more nearly represented by equation 15b. The deviations of the remaining equations were consideraly higher, especially with increasing solids concentration. Equations 12 and 15a appeared not to be applicable at all to these suspensions.

For the glass beads-water system the analytical expressions predict very nearly the same values for each concentration considered. This is to be expected since the thermal conductivity of glass is less than two times that of the water gel. This narrows the range over which the suspension thermal conductivities may vary. For the metal-in-grease suspensions, the greater difference in individual phase thermal conductivities afforded a wider latitude for suspension thermal conductivity variation.

As is evident, the deviation of any one particular equation can be extremely high. Furthermore, the equation whose derivation seems to describe best the physical situation does not necessarily give the best results. An example of this is the results for the spherical aluminum suspensions. This system fits almost perfectly the assumptions leading to equation 11. The experimental results, however, followed almost exactly equation 15b, the derivation of which included no relationship to spherical particles whatever. Thus it is difficult to determine which equation should be used to predict suspension thermal conductivities. In view of their theoretical developments, equations 11, 12, and 13 should be more nearly correct. These equations were developed on rather rigorous statistical arguments which

approximate the actual physical situation of a suspension, and they were not limited with respect to solids composition. In using them, deviations up to 50 per cent from the correct result are probable for solids composition around 0.5 volume fraction.

Two significant conclusions can be drawn from the comparisons. One is that particle shape is of importance in determining suspension thermal conductivities and the other is that particle size distribution also is of importance. The manner in which these two variables are treated mathematically has produced the differences noted.

Upon examining plots of experimentally determined thermal conductivities vs. the suspended phase composition, it is evident that an appropriate relationship with which to attempt a correlation is an exponential one. Efforts to fit such curves with a purely exponential function, however, were not successful. The data could be represented either in the very concentrated regions or when the compositions were very dilute, but not both. Further examination of the experimental data showed that for low compositions of the suspended phase the functional relationship was more nearly that of a polynomial and for the higher compositions an exponential function was more applicable. From this observation the relationship

$$K_m = (1 + av_d + bv_d) \exp (cv_d)^* \qquad (35)$$

was devised where a, b, and c are arbitrary constants, K_m is the ratio, $\frac{k_m}{k_c}$, of the mixture thermal conductivity to that of the continuous phase, and v_d is the dispersed phase composition by volume. For values of v_d

*The symbol "exp" means e, the natural logarithm base, raised to the power appearing in the parenthesis following.

approaching zero, the term e^{cv_d} approaches unity and the functional behavior approaches that of the polynomial; for relatively larger values of v_d approaching unity, the functional behavior is dominated by the exponential expression. Thus this function, in brief, has the properties desired. A series of calculations was made to test the applicability of this equation. The results, tabulated in Table XVI, seem to be very promising. As can be seem the empirically determined equations reproduced the data very closely. Hence it was concluded that this equation was most applicable for fitting conductivity data.

The investigation of this approach was carried further by studying the relationship of the empirical constants. Figure 9 shows how these constants varied with K_d, the ratio of the thermal conductivity of the dispersed phase to that of the continuous phase. From these results, it can be seen that the constants are interdependent and, as expected, are very strongly influenced by changes in K_d. Further, since the zinc particles were almost identical in size to the irregular aluminum particles, points for suspensions made with these powders should have followed the same curve. Thus lines joining these points were assumed to exist. The exact position of the lines could not be determined due to the shortage of data but their general behavior should have been represented.

By consideration of the properties of a suspension having $K_d = 1$, the construction of the curves can be continued. A system composed of components such that $K_d = 1$ means that both phases have the same thermal conductivity. Thus the suspension thermal conductivity would have to be independent of composition, i.e., $K_m = 1$, which means also that a, b, and c must be zero. Therefore, the curves were extended smoothly to include

TABLE XVI

COMPARISON OF EXPERIMENTAL DATA FOR SUSPENSIONS WITH COMPUTATIONS FROM PROPOSED EMPIRICAL EQUATION

Irregular Zinc			Irregular Aluminum			Spherical Aluminum		
Volume Fraction Zinc	Thermal Conductivity (BTU/Hr Ft °F) Exp.[a]	Cal.[b]	Volume Fraction Aluminum	Thermal Conductivity (BTU/Hr Ft °F) Exp.[a]	Cal.[c]	Volume Fraction Aluminum	Thermal Conductivity (BTU/Hr Ft °F) Exp.[a]	Cal.[d]
0.000	1.000	1.000	0.000	1.000	1.000	0.000	1.000	1.000
0.030	1.006	1.042	0.175	1.272	1.253	0.074	1.105	1.109
0.080	1.094	1.120	0.200	1.335	1.335	0.124	1.184	1.184
0.160	1.294	1.294	0.320	1.847	1.815	0.175	1.283	1.287
0.220	1.429	1.462	0.400	2.324	2.394	0.242	1.434	1.439
0.330	1.894	1.893	0.560	4.806	4.806	0.323	1.691	1.691

[a] Data points obtained from smoothed curve.

[b] Calculated from $K_m = (1 - 0.3510v_d + 2.0000v_d^2)\, e^{1.64v_d}$.

[c] Calculated from $K_m = (1 - 1.9763v_d + 3.1965v_d^2)\, e^{3.00v_d}$.

[d] Calculated from $K_m = (1 - 2.1118v_d + 2.1851v_d^2)\, e^{3.50v_d}$.

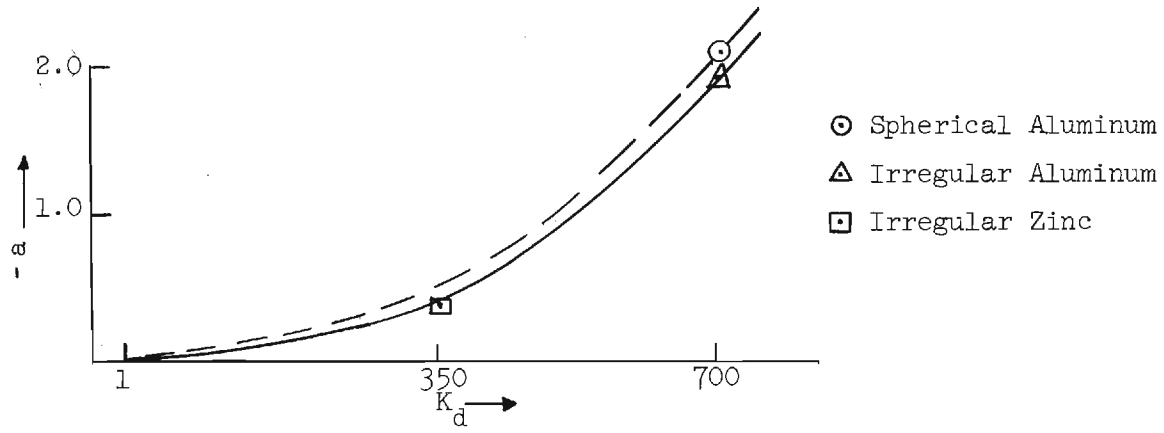

(a) Variation of a with K_d.

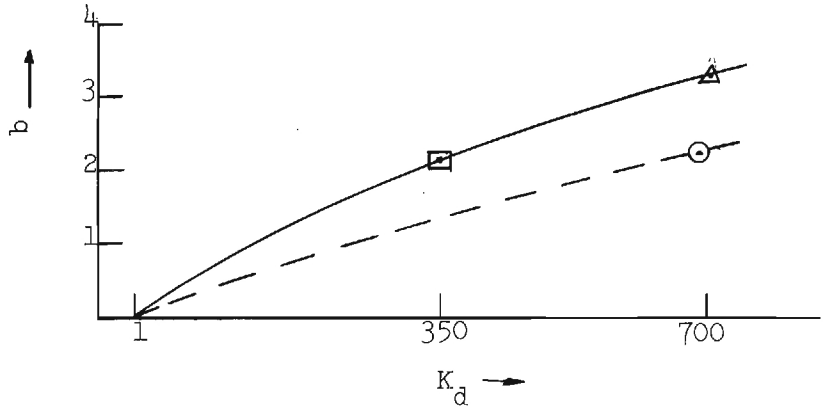

(b) Variation of b with K_d.

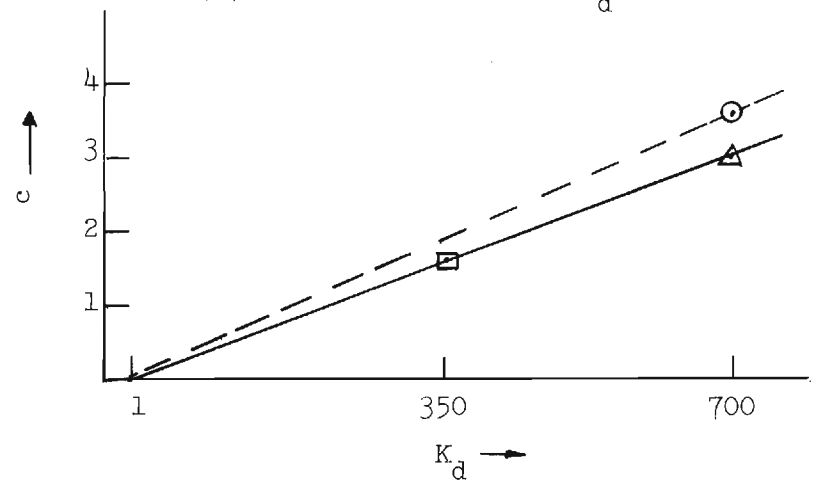

(c) Variation of c with K_d.

Figure 9. Empirical Constants for Equation 35 as Functions of the Ratio of the Pure Phase Thermal Conductivities, K_d.

$K_d = 1$. Construction, however, could not be continued below this value of K_d since there are no experimental data in the region and no theoretical limitations that could be imposed. Since a curve representing the thermal conductivity of such a system would decrease with increase in particulate-phase concentration, all three constants undergo a sign change at $K_d = 1$.

In addition to constructing a curve through points corresponding to suspensions prepared from irregular particles, a similar curve could also be drawn through the points for spherical aluminum powder suspensions. This curve was located on the basis that all curves must go through a common point at $K_d = 1$ and that the divergence of these curve due to differences in particulate shape are very nearly proportional to K_d. Hence the dotted curve for spherical particles was sketched smoothly from the common point at $K_d = 1$ to the single data point at $K_d = 700$. Although the exact position of this curve is not established from this limited amount of data, its general behavior is indicated.

In constructing the empirical relationships for the constants in equation 35, it should be noted that considerable dependence was made on previous conclusions in this report that particle size and particle surface properties did not affect the thermal conductivity of the suspension. These conclusions demand that the thermal conductivity of any system be uniquely determined by the particle shape and the ratio between the pure phase thermal conductivities. Thus the points on the curves in Figure 9 were considered unique and were interpreted as determined by the shape of the suspended particle and by K_d. It is further noted, however, that since the proposed equation and the evaluation of its constants were empirical, this development should be pursued by analyzing other systems containing particles of

similar size distribution, even though particle size should not affect the relationship. This would lend additional strength to the development by avoiding any unnecessary assumptions.

B. Emulsions

From plots of the results presented for emulsions in Tables VIII through XI, it is immediately obvious that within the limits of reliability of data the thermal conductivities of the emulsified systems varied essentially linearly with compositions between the thermal conductivities of the pure phases. These results are in agreement with those of Wang and Knudsen,[28] who performed experimental investigations of several other oil-water systems.

The linear variation of emulsion thermal conductivity with phase composition is the maximum value theoretically possible. This relationship is expressed by

$$K_m = (1 - v_d) + v_d K_d \tag{36}$$

where K_m is the ratio $(\frac{k_m}{k_c})$ of the mixture thermal conductivity to that of the continuous phase,

K_d is the ratio $(\frac{k_d}{k_c})$ of the dispersed phase thermal conductivity to that of the continuous phase,

and v_d is the dispersed phase composition by volume.

The equation can also be shown to represent the heat flow through an idealized model consisting of uniform filaments of each phase arranged parallel to the direction of heat flow. The minimum theoretical thermal conductivity, on the other hand, is given by

$$\frac{1}{K_m} = (1 - v_d) + \frac{v_d}{K_d} \tag{37}$$

This expression also represents the overall thermal conductivity if alternating layers of each phase arranged perpendicular to the direction of heat flow are assumed. Other derived equations give results between these extremes and are based on numerous assumptions of shape, size, and orientation of the dispersed phase. Since emulsified systems can be accurately described as small spherical droplets of one composition dispersed in a continuous phase, such systems should be readily correlated. Predicted values are lower than the experimental ones, however. That most derived expressions do not fit the experimental data more closely is probably due to the series nature of the solutions. Most of the derivations, as discussed in the section on theoretical background, represent one or two terms of an infinite series. It is suspected that the evaluation of more terms of these series would produce better results; however, the equations as presented give results within 15 per cent of the experimental values. This can be seen from the data in Tables XVII through XX.

It might, at first, not be expected that emulsion thermal conductivities should vary linearly with composition. A brief consideration of the properties of the general heat conduction equation shows that this is true, however. Consider the two neighboring regions indicated in the upper drawing of Figure 10. Let the thermal conductivity of component A be many times larger than that of component B. The temperature of the upper surfaces are the same. Now, since the thermal conductivity of component A is large, there is little temperature drop across its domain and the temperature of the adjoining surface between A and B is very nearly T_s, the upper surface temperature. Such a condition gives rise to two dimensional heat conduction as shown in the lower drawing of Figure 10. For this case the heat

TABLE XVII

COMPARISON OF EXPERIMENTAL RESULTS AND ANALYTICAL COMPUTATIONS FOR CARBON TETRACHLORIDE-WATER EMULSIONS*

Data Source	Thermal Conductivity (BTU/Hr Ft °F) for Weight Fractions and, in Parentheses, Corresponding Volume Fractions of				
	0.00 (0.00)	0.20 (0.14)	0.40 (0.30)	0.60 (0.49)	0.80 (0.59)
Experimental	0.328	0.290	0.278	0.195	0.204
Calculated, eq. No. 1	0.360	0.314	0.266	0.215	0.190
Calculated, eq. No. 5	0.360	0.314	0.264	0.210	0.186
Calculated, eq. No. 7	0.360	0.314	0.262	0.208	0.184
Calculated, eq. No. 8	0.360	0.314	0.266	0.212	0.194
Calculated, eq. No. 9	0.360	0.213	0.262	0.203	0.174
Calculated, eq. No. 13a	0.360	0.324	0.282	0.233	0.207
Calculated, eq. No. 13b	0.360	0.264	0.202	0.158	0.142

*Equations No. 10, 11, 12 and 16 not applicable in this system.

TABLE XVIII

COMPARISON OF EXPERIMENTAL RESULTS AND ANALYTICAL COMPUTATIONS FOR HEXANE-WATER EMULSIONS*

Data Source	Thermal Conductivity (BTU/Hr Ft °F) for Weight Fractions and, in Parentheses, Corresponding Volume Fractions of						
	0.00 (0.00)	0.20 (0.28)	0.30 (0.39)	0.40 (0.50)	0.50 (0.60)	0.60 (0.70)	0.70 (0.78)
Experimental	0.352	0.281	0.255	0.214	0.213	0.165	0.147
Calculated, eq. No. 1	0.360	0.232	0.197	0.167	0.145	0.125	0.111
Calculated, eq. No. 5	0.360	0.261	0.225	0.193	0.166	0.141	0.122
Calculated, eq. No. 7	0.360	0.262	0.227	0.193	0.165	0.140	0.123
Calculated, eq. No. 8	0.360	0.236	0.227	0.197	0.165	0.135	0.109
Calculated, eq. No. 9	0.360	0.259	0.222	0.191	0.156	0.126	0.103
Calculated, eq. No. 13a	0.360	0.280	0.250	0.215	0.192	0.165	0.143
Calculated, eq. No. 13b	0.360	0.180	0.151	0.129	0.115	0.103	0.095

*Equations No. 10, 11, 12 and 16 are not applicable in this system.

TABLE XIX

COMPARISON OF EXPERIMENTAL RESULTS AND ANALYTICAL COMPUTATIONS FOR DIETHYLBENZENE-WATER EMULSIONS*

Data Source	Thermal Conductivity (BTU/Hr Ft °F) for Weight Fractions and, in Parentheses, Corresponding Volume Fractions of			
	0.00 (0.00)	0.20 (0.23)	0.40 (0.44)	0.60 (0.64)
Experimental	0.352	0.305	0.259	0.217
Calculated, eq. No. 1	0.360	0.283	0.221	0.169
Calculated, eq. No. 5	0.360	0.282	0.217	0.166
Calculated, eq. No. 7	0.360	0.298	0.241	0.187
Calculated, eq. No. 8	0.360	0.282	0.216	0.150
Calculated, eq. No. 9	0.360	0.280	0.212	0.151
Calculated, eq. No. 13a	0.360	0.298	0.241	0.187
Calculated, eq. No. 13b	0.360	0.212	0.154	0.122

*Equations No. 10, 11, 12 and 16 not applicable in this system.

TABLE XX

COMPARISON OF EXPERIMENTAL RESULTS AND ANALYTICAL COMPUTATIONS FOR TURPENTINE-WATER EMULSIONS*

Data Source	Thermal Conductivity (BTU/Hr Ft °F) for Weight Fractions and, in Parentheses, Corresponding Volume Fractions of				
	0.00 (0.00)	0.20 (0.22)	0.40 (0.43)	0.60 (0.63)	0.80 (0.82)
Experimental	0.352	0.340	0.268	0.200	0.164
Calculated, eq. No. 1	0.360	0.295	0.240	0.192	0.150
Calculated, eq. No. 5	0.360	0.294	0.236	0.190	0.150
Calculated, eq. No. 7	0.360	0.294	0.236	0.190	0.150
Calculated, eq. No. 8	0.360	0.295	0.239	0.188	0.138
Calculated, eq. No. 9	0.360	0.292	0.230	0.174	0.121
Calculated, eq. No. 13a	0.360	0.306	0.255	0.206	0.160
Calculated, eq. No. 13b	0.360	0.246	0.189	0.155	0.132

*Equations No. 10, 11, 12 and 16 not applicable in this system.

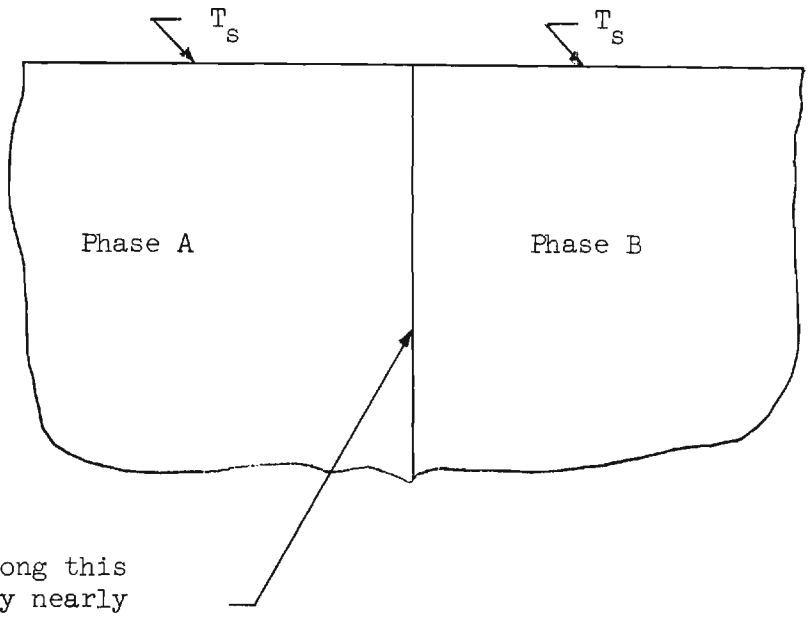

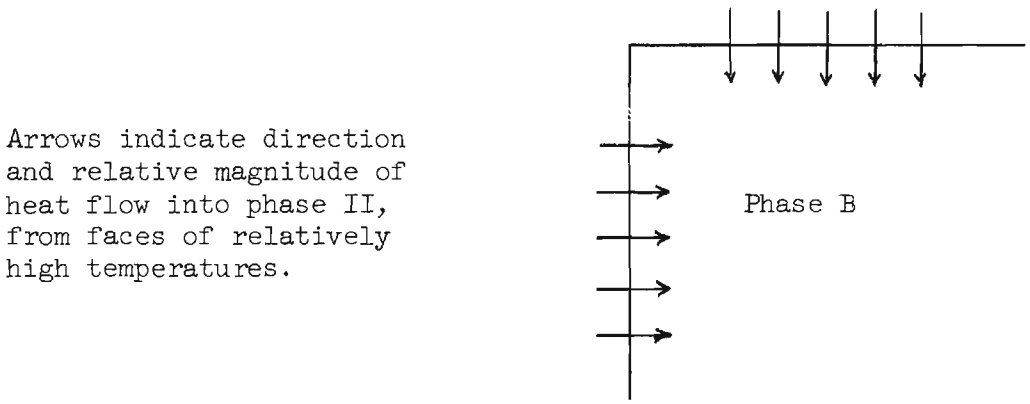

Figure 10. Pictorial Representation of Heat Flow Through Two Adjoining Phases, the Thermal Conductivities of Which Differ by Orders of Magnitude.

flow is described by

$$\frac{\partial^2 t}{\partial x^2} + \frac{\partial^2 t}{\partial y^2} = 0 \tag{38}$$

The solution to this differential equation is nonlinear, and the temperature distribution within each phase is highly dependent upon the other phase material.

When the thermal conductivities of both phases are nearly equal, the temperature distribution along the interface is almost equally dependent on the thermal behavior in both phases and is not much different from the vertical temperature distribution within each phase. This condition gives rise to essentially unidirectional heat conduction as is qualitatively indicated in Figure 11. The temperature field here is governed essentially by the equation

$$\frac{\partial^2 t}{\partial x^2} = 0 \tag{39}$$

the solution to which is linear, and the thermal behavior within each phase is determined largely by its own properties. This relationship is exact when the thermal conductivities of both phases are equal.

To calculate the thermal conductivity of the system, the thermal behavior of both phases and the net heat conducted vertically through both phases must be evaluated and added together. From the argument presented above, it can be seen that for phases having extremely different thermal conductivities, the lateral exchange between the two phases is very significant. When the thermal conductivities are nearly the same this lateral exchange of heat becomes negligible. For the latter it can be shown that

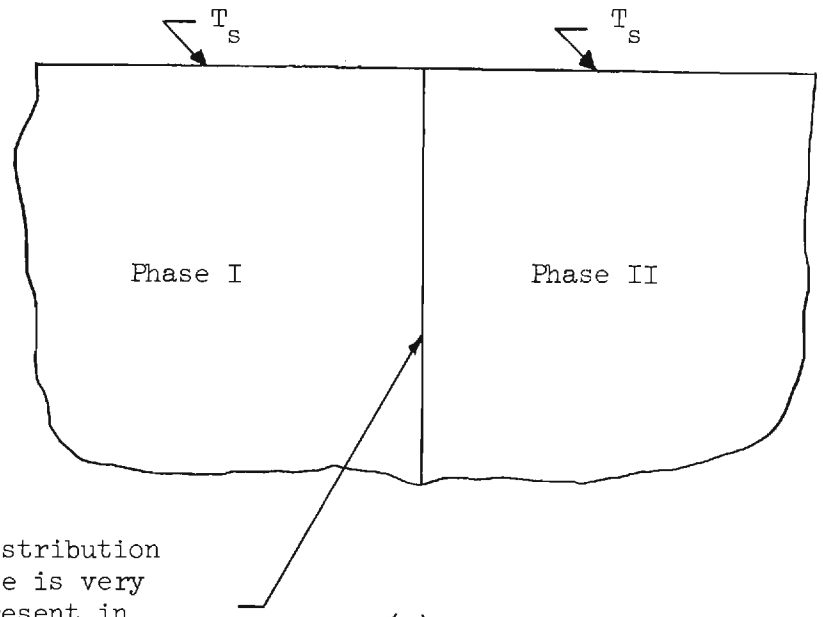

Temperature distribution along interface is very nearly that present in both phases.

(a)

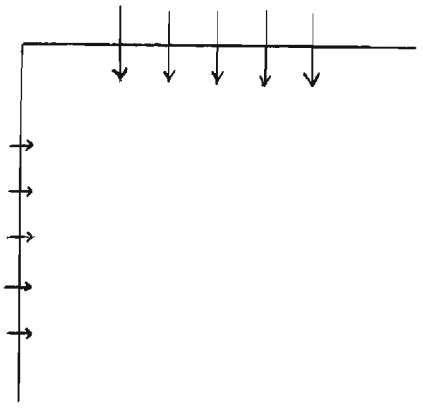

Arrows indicate direction and relative magnitude of heat flow into phase II from upper and side faces.

(b)

Figure 11. Pictorial Representation of the Heat Flow Through Two Adjoining Phases, the Thermal Conductivities of which are Nearly Equal.

the suspended particles may be rearranged.

As shown in the upper portion of Figure 12, the dispersed particles are randomly distributed. In an emulsion region of thickness equal to the average particulate diameter the heat flow is steady and unidirectional and the temperature across each of the particulate faces is constant. Also, as stated before, the behavior of each dispersed particle contained between these two imaginary planes is independent of the surrounding medium. Therefore, since the temperature at the upper and lower faces of each particulate is not affected by the particulate's position within the region, the particulates may be moved at will. This being true, all particles in a given section of emulsion may be shifted so that when this is done for all similar regions the suspended phase forms a continuous filament through the suspension, as shown in the lower drawing of Figure 12.

With the two phases arranged in filaments and with negligible heat exchange between the filaments, the heat flux through each phase is

$$q_c = k_c\left(\frac{dt}{dx}\right)_c \qquad \text{and} \qquad q_d = k_d\left(\frac{dt}{dx}\right)_d \tag{40a,40b}$$

where the subscripts c and d refer to the continuous and dispersed phases, respectively. The total heat transferred through the mixture is

$$k_m A_m \frac{dt}{dx} = k_c A_c \frac{dt}{dx} + k_d \frac{dt}{dx} \tag{41a}$$

or

$$k_m = k_c \frac{A_c}{A_m} + k_d \frac{A_d}{A_m} \tag{41b}$$

where A is the area through which heat transfer occurs. Equation 41b is equivalent to

$$k_m = k_c v_c + k_d v_d \tag{42a}$$

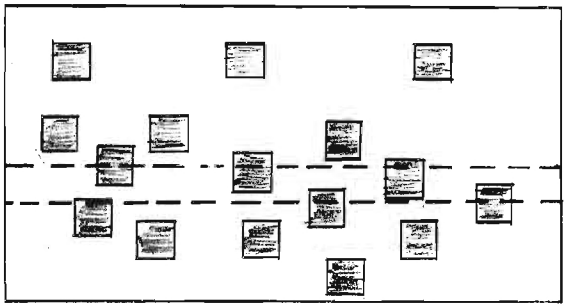

a. Random Arrangement of Dispersed Droplets.

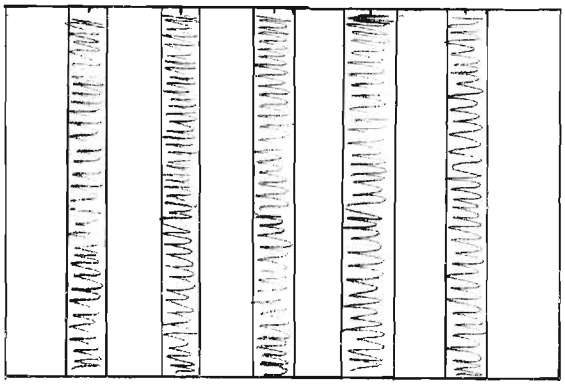

b. Particles Repositioned and Collected into Continuous Filaments.

Figure 12. Pictorial Representation of the Possible Rearrangement of Two-Phases When Their Thermal Conductivities Are Not Greatly Different.

or $$K_m = (1 - v_d) + K_d v_d \qquad (42b)$$

Thus, the equivalent thermal conductivity is a linear function of the dispersed composition.

The above relationships are limiting expressions. They are exact only when the thermal conductivity of both phases are equal and are approximate for cases in which the pure phase thermal conductivities approach each other. Their utility, however, is well substantiated by the experimental data presented herein which represent cases where the pure phase thermal conductivities differed by factors of as much as 4; excellent agreement with equation 42b was still obtained. Thus it is considered that equation 42b is adequate for predicting emulsion thermal conductivities. This result should be universally applicable to a great variety of emulsion systems since most pure liquid thermal conductivities rarely differ by more than a factor of 4. Emulsions containing one of the liquid metals, e.g., mercury, gallium, or thallium, would constitute the major exceptions.

C. Powder Beds

The thermal behavior of powder beds was investigated by studying a series of gas-glass beads systems in which the gas and the size of the glass beads were varied. This permitted the measurements to reflect changes in the most important of the variables involved in powder bed heat transfer, for it has been shown by previous investigators that the thermal conductivity of powder bed systems is largely a function of particle shape and size, intervening gas pressure, and the thermal properties (including radiation) of both phases. These quantitites are, therefore, basically the minimum needed to define a system. The data have been used to study the

reliability of the various theoretical developments for predicting the thermal conductivity of powder beds.

Although numerous mechanisms of heat transfer are understood, reliable calculations for powder bed thermal conductivity are difficult to develop from a purely theoretical point of view. For readily describing beds, such as those containing only spherical particles, a theoretical calculation can be made. Even here, however, empirical guidance is highly desirable. Table XXI presents a series of computed thermal conductivities and the corresponding measured values. As shown, the more reliable expressions are in part empirical. Equation 19, an example of a purely theoretical approach, gives results that are inferior to those of the semiempirical calculations. Equation 24, on the other hand, gives results superior to any other development. Equations 25 and 26 predict better values than equation 19, but are still incorrect by approximately an order of magnitude. It is thought that equations 27a, 27b, and 27c would give results comparable to those of equation 24; they could not be considered, however, because the empirical constants ϕ and δ were not know for the systems investigated. From the results obtained, equation 24 appears, at least for the present, to be the best available for normal temperature conditions.

TABLE XXI

COMPARISON OF EXPERIMENTAL RESULTS AND ANALYTICAL COMPUTATIONS FOR GAS-GLASS BEADS SYSTEMS

System	Experimental Values (BTU/Hr Ft ^{o}F)	Computed Thermal Conductivity Values from Equations* (BTU/Hr Ft ^{o}F)		
		19	24	26
Air-glass beads 30μ average diameter	0.106	0.005	0.114	0.011
Air-glass beads 290μ average diameter	0.121	0.005	0.114	0.011
Air-glass beads 340μ average diameter	0.125	0.005	0.114	0.011
Air-glass beads 750μ average diameter	0.128	0.005	0.114	0.011
Helium-glass beads 750μ average diameter	0.130	0.005	0.662	0.067
Natural gas-glass beads 36μ average diameter	0.115	0.005	0.200	0.012
Natural gas-glass beads 290μ average diameter	0.137	0.005	0.200	0.012
Natural gas-glass beads 340μ average diameter	0.146	0.005	0.200	0.012
Natural gas-glass beads 750μ average diameter	0.148	0.005	0.200	0.012

*The results for equation 25 are not tabulated since they are identical to those of equation 26.

VI. CONCLUSIONS

This research pertained to thermal conductivities exhibited by two-phase systems, one phase of which was uniformly dispersed in particulate form throughout the other. Three types of dispersions--suspensions (one solid phase and one liquid phase), emulsion (two immiscible liquid phases), and powder beds (one solid phase and one gas phase)--were investigated. From the results the following conclusions are believed justified.

1. The thermal conductivity of a suspension is independent of particle size if the particles' surfaces are wet by the fluid, if the particles are not porous, and if the system is sufficiently large for the dispersion to be considered uniform. With porous particles, air or other gas (a third phase) may be entrapped in the pores and change the thermal behavior of the particles. This indirecly makes the specific surface area an additional characterization factor.

2. The thermal conductivity of a suspension is uninfluenced by small quantities of a wetting or dispersing agent provided the solid phase is wet by the liquid. This results from the fact that a wetted surface has negligible thermal resistance.

3. The thermal conductivity of a suspension is a function of particle shape. Irregular particles produce suspensions with higher thermal conductivities than do spherical particles, for example.

4. The empirical equation

$$\frac{k_m}{k_c} = (1 + av_d + bv_d) \exp (cv_d)$$

gives an excellent representation of the thermal conductivity of a

suspension as a function of dispersed phase composition. In this equation, k_m/k_c is the ratio of the thermal conductivity of the mixture to that of the continuous phase and v_d is the dispersed phase composition by volume. The constants a, b, and c are functions of the ratio of the dispersed phase thermal conductivity, k_d, to that of the continuous phase conductivity k_c with particle shape as a parameter.

5. Of the previous equations estimating suspension thermal conductivity, equations 11, 12, and 13 are considered in general the more reliable. These expressions were derived for spheres and for rods oriented in both two and three dimensions, are based on a statistically sound argument, and are not restricted to small dispersed-phase compositions as are most other developments. For most systems composed of materials having pure phase thermal conductivity ratios of over 300, equation 18 should be valid. Its estimate, however, may be in error by as much as 100 per cent for higly concentrated dispersions.

6. The thermal conductivity of an emulsion is linearly related (within experimental error) to the dispersed phase composition. This means that equation 42b is quite reliable for systems in which the pure phase thermal conductivities are different by ratios of no more than four. This includes essentially all emulsions.

7. The thermal conductivity of a powder bed is still best determined by equations having empirical correction factors. Equation 24 appears to be the most generally applicable for normal temperature conditions. Equations 25 and 26 seem to give results correct within an order of magnitude.

VII. RECOMMENDATIONS

Much of the effort expended on the thermal conductivity of two-phase dispersions has been devoted to theoretical analyses of the mechanisms involved. A number of expressions, therefore, have been proposed, but experimental results have shown that most of them are applicable only to special cases. The mechanisms actually involved are so complex that the simplified conditions of the proposed mathematical models are almost never met, and, furthermore, the deviations from the mathematical models are not calculable. In view of this, much reliance must still be placed on empirical solutions.

Except, perhaps, in cases where extreme variations in particulate properties are involved, this investigation has shown that the thermal conductivity of two-phase systems is a strong function of particle shape and the pure component thermal conductivities but is weakly (if not negligibly) affected by particle size and particle surface properties. It has been further shown that an empirical equation is readily adaptable to describing experimental results and that the empirical constants in this equation are orderly related to particle shape and the ratio of component thermal conductivities. In view of these results, it is recommended that this approach be pursued further with the collection of additional experimental data to define and establish the uniqueness of these empirical constants.

Respectfully submitted:

Clyde Orr, Jr.
Project Director

Approved:

Wyatt C. Whitley, Chief
Chemical Sciences Division

VIII. APPENDIX

A. References

1. J. C. Maxwell, Electricity and Magnetism, Vol. 1, 3rd. ed., Oxford University Press, London (1892).

2. Lord Rayleigh, "On the Influence of Obstacles in Rectangular Order upon the Properties of a Medium," Phil. Mag. 34, 481-502 (1925).

3. I. Runge, "Zur elektrischen Leitfähigkeit metallischer Aggregate," Zeit. Teck. Phys. 6, 61-8 (1925).

4. D. A. G. Bruggerman, "Berechnung verschiedener physikalischer Konstanten von heterogenen Substanzen," Ann. Phys. 24, 636-64 (1935).

5. R. E. Meredith, Studies on the Conductivities of Dispersions, Ph.D. Thesis, Univ. of California, Berkeley, California (1959).

6. H. C. Burgers, "Das Leitvermögen verdünnter mischkristallfreier Legierungen," Phys. Zeit. 20, 73-5 (1919).

7. O. Wiener, "Die Theorie des Mischkörpers für das Feld der stationären Stromung," Abd. d. Leipz. Akad. 32, 509 (1912).

8. K. Lichtenecker, "Die Dielektrizitätkonstante natürlicher und kunstlicher Mischkörper," Phys. Zeit. 27, 115-58 (1926).

9. J. B. Jefferson, O. W. Witzell, and W. L. Sibitt, "Thermal Conductivity of Graphite-Silicone Oil and Graphite-Water Suspensions," Ind. Eng. Chem. 50, 1589 (1958).

10. H. W. Russell, Principles of Heat Flow in Porous Insulators," J. Am. Ceramic Soc. 18, 1-4 (1935).

11. R. G. Deissler and C. S. Eian, Investigation of Effective Thermal Conductivities of Powders, National Advisory Committee for Aeronautics, RM E52C05, (1952).

12. H. S. Strickler, "Thermal Conductivity of Solids and Fluids from Studies of Aggregate Matter," J. Chem. Phys. 20, 1333-4 (1952).

13. H. S. Strickler, "Thermal Conductivity of Granulated Beds," Ind. Eng. Chem. 46, 828 (1954).

14. W. Woodside, "Calculation of the Thermal Conductivity of Porous Media," Can. J. Phys. 36, 815-23 (1958).

15. R. G. Deissler and J. S. Boegli, "Effective Thermal Conductivities of Powders in Various Gases," Trans. ASME 80, 1417-25 (1958).

16. M. N. Marathe and G. S. Tenkolkar, "Measurement of Thermal Conductivity of Powders," Trans. Indian Inst. Chem. Engrs. VI, 90-104 (1953-54).

17. W. Schotte, "Thermal Conductivity of Packed Beds," A.I.Ch.E. Journal 6, 63-7 (1960).

18. S. Yagi and D. Kunii, "Studies on Effective Thermal Conductivities in Packed Beds," A.I.Ch.E. Journal 3, 373-81 (1957).

19. M. J. Laubitz, "Thermal Conductivity of Powders," Can. J. Phys. 37, 798-808 (1959).

20. M. Kimura, "Effective Thermal Conductivities of Packed Beds," Chem. Eng. (Japan) 21, 473-80 (1957).

21. S. Sugiyama and M. Fujitsu, "Effective Thermal Conductivities in Packed Beds," Chem. Eng. (Japan) 24, 12-19 (1960).

22. W. E. Ranz, "Friction and Transfer Coefficients for Single Particles and Packed Beds," Chem. Eng. Prog. 48, 247-53 (1952).

23. J. L. Weininger and W. G. Schneider, "Thermal Conductivity of Granular Beds Filled with Compressed Gases," Ind. Eng. Chem. 43, 1229-33 (1951).

24. B. C. Sakiadis and J. Coates, "Studies of Thermal Conductivity of Liquids. Supplement to Part I. A., Louisiana State University, Eng. Expt. Sta. Bull 48, Baton Rouge, La. (1954).

25. O. K. Bates, "Thermal Conductivity of Liquids," Ind. Eng. Chem. 29, 435-36 (1933).

26. C. Orr, Jr. and J. M. DallaValle, "Heat-Transfer Properties of Liquid-Solid Suspensions," Heat Transfer, Symposium Series No. 9 50, 29-45 (1954).

27. Chemical Engineers' Handbook (J. H. Perry, editor-in-chief), McGraw-Hill Company, Inc., New York (1950).

28. R. H. Wang and J. G. Knudsen, "Thermal Conductivity of Liquid-Liquid Emulsions," Ind. Eng. Chem. 50, 1667-70 (1958).

B. Experimental Data

TABLE XXII

EXPERIMENTAL DATA FOR PURE WATER AS A HEAT TRANSFER MEDIUM

Thermocouple Data		Temperature (°C)						
		Experiment I				Experiment II		
Position	Spacing (Cm)	Run 1	Run 2	Run 3	Run 4	Run 1	Run 2	Run 3
Hot plate	--	63.18	63.20	63.20	63.20	59.50	59.50	59.50
1	4.39	52.10	52.10	52.30	52.20	52.70	52.70	52.60
2	3.69	45.30	45.35	45.50	45.40	45.60	45.60	45.60
3	3.15	39.60	39.60	39.80	39.80	39.50	39.55	39.60
4	2.51	32.65	32.65	32.75	32.80	32.90	33.00	33.00
5	1.87	26.10	26.10	25.90	25.90	26.10	26.20	26.15
6	1.19	18.50	18.40	18.40	18.40	18.70	18.75	18.75
7	0.57	11.60	11.50	11.50	11.55	11.90	11.90	11.90
Cold plate	0.00	3.10	3.05	3.10	3.05	3.60	3.55	3.55

TABLE XXIII

EXPERIMENTAL DATA FOR GLASS BEADS-WATER (GELLED) SUSPENSIONS

A. Fluid Space Data

Distance of Thermocouple Above the Comparison Block (Cm)	Temperature in °C for Weight Per Cent Glass Compositions of*				
	0%	25%	37%	50%	71%
4.36	24.15	53.50	52.45	52.60	50.60
3.68	46.40	45.65	44.80	44.05	44.05
3.11	40.35	39.65	38.75	38.75	37.55
2.50	33.45	32.75	31.95	31.95	31.95
1.38	20.75	20.15	19.65	20.05	20.35
0.63	12.70	12.30	11.90	12.80	12.65

B. Comparison Block Data

Thermocouple Separation	Temperature Difference Across Block in °C for Weight Per Cent Glass Bead Compositions of*				
	0%	25%	37%	50%	71%
11.43 cm measured axially across block	2.65	2.65	2.60	2.50	2.62

*Average Temperatures from three separate determinations.

TABLE XXIV

EXPERIMENTAL DATA FOR ZINC A-GREASE SUSPENSIONS

A. Fluid Space Data

Distance of Thermocouple Above Comparison Block (Cm)	Temperatures* in °C for Weight Per Cent Zinc Compositions of								
	0%	20%	40%	60%	70%	75%	80%	85%	90%
4.36	52.80	52.50	52.60	51.70	52.60	52.00	52.05	51.50	52.50
3.68	44.70	44.50	45.10	44.10	44.75	44.45	44.40	44.10	44.60
3.11	38.20	38.10	38.30	37.80	38.75	38.35	38.00	37.70	38.50
2.50	31.00	30.80	31.30	30.60	31.40	31.30	30.90	30.55	31.50
1.38	18.00	18.15	18.75	18.20	18.90	19.20	18.50	18.30	19.80
0.63	10.00	10.45	10.80	10.60	11.00	11.40	10.75	10.75	12.30

B. Comparison Block Data

Thermocouple Separation	Temperature Difference Across Block in °C for Weight Per Cent Zinc Compositions of								
	0%	20%	40%	60%	70%	75%	80%	85%	90%
11.43 cm measured axially across block	1.25	1.44	1.53	1.63	1.94	2.20	2.45	2.77	3.68

*Average value from 8 to 10 determinations.

TABLE XXV

EXPERIMENTAL DATA FOR ZINC B-GREASE SUSPENSIONS

A. Fluid Space Data

Distance of Thermocouple Above Comparison Block (Cm)	Temperature* in °C for Weight Per Cent Zinc Compositions of					
	0%	50%	60%	70%	80%	90%
4.56	52.40	52.20	53.00	50.60	50.65	51.20
3.68	44.45	44.50	45.30	43.20	43.20	43.85
3.11	37.95	38.40	38.70	37.30	37.30	37.75
2.50	30.55	31.35	32.20	30.70	30.70	30.90
1.38	18.05	19.25	20.05	19.25	18.25	19.30
0.63	9.95	11.05	11.85	11.15	10.85	12.05

B. Comparison Block Data

Thermocouple Separation	Temperature Difference Across Block in °C for Weight Per Cent Zinc Compositions of					
	0%	50%	60%	70%	80%	90%
11.43 cm measured axially across block	1.30	1.67	1.70	1.81	2.23	3.42

*Average value from 8 to 10 determinations.

TABLE XXVI

EXPERIMENTAL DATA FOR ZINC B-GREASE SUSPENSIONS BEFORE ADDITION OF A SURFACE ACTIVE AGENT

A. Fluid Space Data

Distance of Thermocouple Above Comparison Block (Cm)	Temperatures* in °C for Weight Per Cent Zinc Compositions of					
	0%	20%	40%	60%	70%	80%
4.36	52.20	52.25	52.50	51.80	51.35	51.40
3.68	44.75	44.95	44.60	44.10	44.08	44.80
3.11	38.55	38.65	38.15	37.70	37.10	37.45
2.50	30.90	31.35	30.90	30.20	30.70	31.15
1.38	18.80	19.00	18.55	18.60	18.85	19.35
0.63	10.35	10.20	10.30	10.61	11.11	11.71

B. Comparison Block Data

Thermocouple Separation	Temperature Difference Across Block in °C for Weight Per Cent Zinc Compositions of					
	0%	20%	40%	60%	70%	80%
11.43 cm measured axially across block	1.17	1.24	1.37	1.49	1.70	2.22

*Average value from 8 to 10 determinations.

TABLE XXVII

EXPERIMENTAL DATA FOR ZINC B-GREASE SUSPENSIONS WITH A SURFACE ACTIVE AGENT

A. Fluid Space Data

Distance of Thermocouple Above Comparison Block (Cm)	Temperature* in °C for Weight Per Cent Zinc Compositions of			
	0%	60%	70%	80%
4.36	52.60	52.05	52.25	52.25
3.68	44.80	44.95	45.10	44.70
3.11	38.35	38.20	38.60	38.20
2.50	31.05	31.70	32.10	31.40
1.38	18.50	19.30	19.35	19.75
0.63	10.26	11.26	11.16	12.15

B. Comparison Block Data

Thermocouple Separation	Temperature Difference Across Block in °C for Weight Per Cent Zinc Compositions of			
	0%	60%	70%	80%
11.43 cm measured axially across block	1.23	1.60	1.68	2.20

*Average value from 8 to 10 determinations

TABLE XXVIII

EXPERIMENTAL DATA FOR IRREGULAR ALUMINUM-GREASE SUSPENSIONS

A. Fluid Space Data

Distance of Thermocouple Above Comparison Block (Cm)	Temperature* in °C for Weight Per Cent Aluminum Compositions of					
	0%	20%	40%	60%	70%	80%
4.36	51.80	51.40	51.45	50.75	51.55	52.15
3.68	45.10	44.65	44.30	43.55	44.15	46.00
3.11	38.40	38.25	38.15	37.90	38.05	40.28
2.50	30.90	31.75	31.90	32.05	31.60	34.10
1.38	18.00	19.30	20.20	21.10	20.60	23.85
0.63	10.18	11.05	12.10	13.28	13.50	18.00

B. Comparison Block Data

Thermocouple Separation	Temperature Difference Across Block in °C for Weight Per Cent Aluminum Compositions of					
	0%	20%	40%	60%	70%	80%
11.43 cm measured axially across block	1.14	1.30	1.50	2.20	2.74	4.05

*Average value from 8 to 10 determinations.

TABLE XXIX

EXPERIMENTAL DATA FOR SPHERICAL ALUMINUM A-GREASE SUSPENSIONS

A. Fluid Space Data

Distance of Thermocouple Above Comparison Block (Cm)	Temperature in °C for Weight Per Cent Aluminum Compositions of					
	0%	20%	30%	40%	50%	60%
4.36	51.60	52.75	52.55	52.60	52.50	52.97
3.68	44.60	45.90	45.75	45.60	45.60	46.30
3.11	37.70	39.15	38.35	35.75	38.80	39.35
2.50	30.50	32.25	31.68	32.15	32.55	32.70
1.38	17.55	19.35	18.95	18.95	19.48	20.02
0.63	9.70	11.75	11.40	11.62	12.05	12.56

B. Comparison Block Data

Thermocouple Separation	Temperature Difference Across Block in °C for Weight Per Cent Aluminum Compositions of					
	0%	20%	30%	40%	50%	60%
11.43 cm measured axially across block	1.12	1.26	1.30	1.42	1.55	1.82

TABLE XXX

EXPERIMENTAL DATA FOR SPHERICAL ALUMINUM B-GREASE SUSPENSIONS

A. Fluid Space Data

Distance of Thermocouple Above Comparison Block (Cm)	Temperature in °C for Weight Per Cent Aluminum Compositions of				
	0%	20%	30%	41.9%	49.7%
4.36	53.05	53.15	53.18	52.95	52.48
3.68	45.70	46.04	46.20	45.85	45.28
3.11	38.75	39.30	39.30	39.10	38.52
2.50	31.80	32.55	32.86	32.45	31.62
1.38	18.68	19.74	19.72	19.98	19.20
0.63	11.10	12.05	11.92	12.50	11.90

B. Comparison Block Data

Thermocouple Separation	Temperature Difference Across Block in °C for Weight Per Cent Aluminum Compositions of				
	0%	20%	30%	41.9%	49.7%
11.43 cm measured axially across block	1.12	1.20	1.25	1.45	1.55

TABLE XXXI

EXPERIMENTAL DATA FOR SPHERICAL ALUMINUM C-GREASE SUSPENSIONS

A. Fluid Space Data

Distance of Thermocouple Above Comparison Block (Cm)	Temperature in °C for Weight Per Cent Aluminum Compositions of				
	20%	30%	40%	50%	55.49%
4.36	53.57	53.40	53.20	52.60	52.58
3.68	46.30	46.40	46.05	45.50	45.70
3.11	39.44	39.40	38.95	38.70	38.75
2.50	32.80	32.68	32.30	31.80	31.98
1.38	19.58	19.85	19.65	19.12	19.28
0.63	12.40	12.60	12.25	11.50	11.70

B. Comparison Block Data

Thermocouple Separation	Temperature Difference Across Block in °C for Weight Per Cent Aluminum Compositions of				
	20%	30%	40%	50%	55.4%
11.43 cm measured axially across block	1.25	1.30	1.40	1.52	1.62

TABLE XXXII

EXPERIMENTAL DATA FOR FLAKE ALUMINUM-GREASE SUSPENSIONS

A. Fluid Space Data

Distance of Thermocouple Above Comparison Block (Cm)	Temperature in °C for Weight Per Cent Aluminum Compositions of				
	0%	20%	30%	40%	50%
4.36	53.15	50.75	48.78	50.95	47.90
3.68	45.75	46.60	46.00	48.55	39.80
3.11	39.10	41.40	42.40	46.40	35.80
2.50	31.85	37.10	40.00	40.54	31.30
1.38	19.15	27.60	30.75	31.90	22.15
0.63	11.85	19.55	23.12	22.35	17.48

B. Comparison Block Data

Thermocouple Separation	Temperature Difference Across Block in °C for Weight Per Cent Aluminum Compositions of				
	0%	20%	30%	40%	50%
11.43 cm measured axially across block	1.17	1.85	2.44	3.46	3.63

TABLE XXXIII

EXPERIMENTAL DATA FOR CARBON TETRACHLORIDE-WATER EMULSIONS

A. Fluid Space Data

Distance of Thermocouple Above Comparison Block (Cm)	Temperature in °C for Weight Per Cent Carbon Tetrachloride Compositions of				
	0%	20%	40%	60%	70%
4.36	52.60	49.35	52.45	54.85	54.95
3.68	46.00	40.45	46.30	49.65	48.00
3.11	39.85	37.00	40.40	43.42	41.75
2.50	32.65	28.80	34.15	36.35	34.50
1.38	20.05	17.35	22.70	23.35	22.10
0.63	12.37	11.22	16.10	14.30	13.80

B. Comparison Block Data

Thermocouple Separation	Temperature Difference in °C Across Block for Weight Per Cent Carbon Tetrachloride Compositions of				
	0%	30%	40%	60%	70%
11.43 cm measured axially across block	2.38	2.02	1.80	1.5	1.5

TABLE XXXIV

EXPERIMENTAL DATA FOR HEXANE-WATER EMULSIONS

A. Fluid Space Data

Distance of Thermocouple Above Comparison Block (Cm)	Temperature in °C for Weight Per Cent Hexane Compositions of						
	0%	20%	30%	40%	50%	60%	70%
4.36	51.00	52.58	50.80	52.80	51.10	48.60	50.90
3.68	44.71	46.20	43.35	46.20	43.88	40.60	42.35
3.11	38.55	38.80	38.75	41.77	37.50	33.33	34.40
2.50	32.22	32.82	30.65	33.85	30.15	25.00	26.25
1.38	20.25	19.92	18.30	19.70	17.60	14.75	12.60
0.63	12.50	11.92	10.75	11.45	10.00	8.67	7.30

B. Comparison Block Data

Thermocouple Separation	Temperature Difference in °C Across Block for Weight Per Cent Hexane Compositions of						
	0%	20%	30%	40%	50%	60%	70%
11.43 cm measured axially across block	2.46	2.05	1.80	1.70	1.55	1.35	1.3

TABLE XXXV

EXPERIMENTAL DATA FOR DIETHYLBENZENE-WATER EMULSIONS

A. Fluid Space Data

Distance of Thermocouple Above Comparison Block (Cm)	Temperature in °C for Weight Per Cent Diethylbenzene Compositions of			
	0%	20%	40%	60%
4.36	51.00	48.85	47.45	50.50
3.68	44.71	42.40	39.12	43.80
3.11	38.55	36.22	33.25	37.10
2.50	32.22	30.05	27.12	30.60
1.38	20.25	17.90	15.60	18.42
0.63	12.50	10.76	8.35	10.40

B. Comparison Block Data

Thermocouple Separation	Temperature Difference in °C Across Block for Weight Per Cent Diethylbenzene Compositions of			
	0%	20%	40%	60%
11.43 cm measured axially across block	2.46	2.06	1.72	1.55

TABLE XXXVI

EXPERIMENTAL DATA FOR TURPENTINE-WATER EMULSIONS

A. Fluid Space Data

Distance of Thermocouple Above Comparison Block (Cm)	Temperature in °C for Weight Per Cent Turpentine Compositions of				
	0%	20%	40%	60%	70%
4.36	51.00	46.50	47.85	50.90	52.10
3.68	44.71	39.85	40.60	44.65	45.20
3.11	38.55	34.65	35.30	38.00	38.30
2.50	32.22	28.75	29.05	31.90	31.25
1.38	20.25	21.20	24.00	19.00	18.20
0.63	12.50	10.35	9.75	11.10	10.45

B. Comparison Block Data

Thermocouple Separation	Temperature Difference in °C Across Block for Weight Per Cent Diethylbenzene Compositions of				
	0%	20%	40%	60%	80%
11.43 cm measured axially across block	2.46	2.19	1.77	1.47	1.27

TABLE XXXVII

EXPERIMENTAL DATA FOR GAS-GLASS BEADS SYSTEMS

System	Temperature Difference Measurements in °C Across		Weight of Glass Beads in Bed (Gm.)
	Powder Bed	Comparison Block	
Air-glass beads 36μ average diameter	56.73	2.07	483
Air-glass beads 290μ average diameter	56.15	2.34	591
Air-glass beads 340μ average diameter	55.97	2.42	630
Air-glass beads 750μ average diameter	56.12	2.48	726
Helium-glass beads 750μ average diameter	56.10	2.51	726
Natural gas-glass beads 36μ average diameter	56.29	2.24	483
Natural gas-glass beads 290μ average diameter	55.77	2.65	593
Natural gas-glass beads 340μ average diameter	55.50	2.80	625
Natural gas-glass beads 750μ average diameter	55.50	2.84	726